Rp-cAMPS Prodrugs Reveal the cAMP Dependence of First-Phase Glucose-Stimulated Insulin Secretion

Frank Schwede,* Oleg G. Chepurny,* Melanie Kaufholz, Daniela Bertinetti, Colin A. Leech, Over Cabrera, Yingmin Zhu, Fang Mei, Xiaodong Cheng, Jocelyn E. Manning Fox, Patrick E. MacDonald, Hans-G. Genieser, Friedrich W. Herberg, and George G. Holz

BIOLOG Life Science Institute (F.S., H.-G.G.), 28199 Bremen, Germany; Departments of Medicine (O.G.C., C.A.L., G.G.H.) and Pharmacology (G.G.H.), State University of New York, Upstate Medical University, Syracuse, New York 13210; Department of Biochemistry (M.K., D.B., F.W.H.), University of Kassel, 34132 Kassel, Germany; Eli Lilly and Company (O.C.), Indianapolis, Indiana 46225; Department of Integrative Biology and Pharmacology (Y.Z., F.M., X.C.), Texas Therapeutics Institute, The Brown Foundation Institute of Molecular Medicine, The University of Texas Health Science Center, Houston, Texas 77030; Department of Pharmacology and the Alberta Diabetes Institute (J.E.M.F., P.E.M.), University of Alberta, Edmonton, Canada AB T6G 2E1

cAMP-elevating agents such as the incretin hormone glucagon-like peptide-1 potentiate glucose-stimulated insulin secretion (GSIS) from pancreatic β-cells. However, a debate has existed since the 1970s concerning whether or not cAMP signaling is essential for glucose alone to stimulate insulin secretion. Here, we report that the first-phase kinetic component of GSIS is cAMP-dependent, as revealed through the use of a novel highly membrane permeable para-acetoxybenzyl (pAB) ester prodrug that is a bioactivatable derivative of the cAMP antagonist adenosine-3′,5′-cyclic monophosphorothioate, Rp-isomer (Rp-cAMPS). In dynamic perifusion assays of human or rat islets, a step-wise increase of glucose concentration leads to biphasic insulin secretion, and under these conditions, 8-bromoadenosine-3′,5′-cyclic monophosphorothioate, Rp-isomer, 4-acetoxybenzyl ester (Rp-8-Br-cAMPS-pAB) inhibits first-phase GSIS by up to 80%. Surprisingly, second-phase GSIS is inhibited to a much smaller extent ($\leq$20%). Using luciferase, fluorescence resonance energy transfer, and bioluminescence resonance energy transfer assays performed in living cells, we validate that Rp-8-Br-cAMPS-pAB does in fact block cAMP-dependent protein kinase activation. Novel effects of Rp-8-Br-cAMPS-pAB to block the activation of cAMP-regulated guanine nucleotide exchange factors (Epac1, Epac2) are also validated using genetically encoded Epac biosensors, and are independently confirmed in an in vitro Rap1 activation assay using Rp-cAMPS and Rp-8-Br-cAMPS. Thus, in addition to revealing the cAMP dependence of first-phase GSIS from human and rat islets, these findings establish a pAB-based chemistry for the synthesis of highly membrane permeable prodrug derivatives of Rp-cAMPS that act with micromolar or even nanomolar potency to inhibit cAMP signaling in living cells. **(*Molecular Endocrinology* 29: 988–1005, 2015)**

Adenosine-3′,5′-cyclic monophosphorothioate, Rp-isomer (Rp-cAMPS) is a synthetic diastereomeric phosphorothioate analog of naturally occurring cAMP, and it is commonly used in cyclic nucleotide research as an antagonist of cAMP-dependent protein kinase (PKA) activation (1). Rp-cAMPS competes with cAMP for binding to the "A" and "B" cyclic nucleotide-binding domains located on PKA regulatory subunits, yet unlike cAMP, it

ISSN Print 0888-8809 ISSN Online 1944-9917
Printed in USA

Received October 16, 2014. Accepted May 8, 2015.
First Published Online June 10, 2015

* F.S. and O.G.C. contributed equally to this work.

Abbreviations: AKAR3, A-kinase activity reporter 3; AM-ester, acetoxymethyl ester; BRET, bioluminescence resonance energy transfer; CRE, cAMP response element; CREB, cAMP response element-binding protein; DMSO, dimethyl sulfoxide; Epac, exchange protein directly activated by cAMP; ESCA-AM, AM-ester of an Epac-selective cAMP analog; ESI-MS, electrospray ionization mass spectrometry; Ex-4, exendin-4; FBS, fetal bovine serum; FL, full length; FRET, fluorescence resonance energy transfer; GDP, guanosine 5′-diphosphate; GEF, guanine nucleotide exchange factor; GLP-1, glucagon-like peptide-1; GLP-1R, GLP-1 receptor; GSIS, glucose-stimulated insulin secretion; IBMX, 3-isobutyl-1-methylxanthine; NMR, nuclear magnetic resonance; pAB, para-acetoxybenzyl; PKA, cAMP-dependent protein kinase; RIP1, rat insulin 1 gene promoter; RIP1-CRE-Luc, RIP1-CRE luciferase assay.

fails to promote PKA holoenzyme dissociation and resultant activation (1). For live-cell studies of PKA signaling, Rp-cAMPS can be introduced into cells by patch clamp dialysis (2, 3) or by plasma membrane permeabilization (4, 5). However, Rp-cAMPS is a poor antagonist of PKA activation when it is administered by the extracellular route due to the fact that the negatively charged thiophosphate moiety of Rp-cAMPS reduces its lipophilicity and membrane permeability (1). Thus, it is imperative that a new cyclic nucleotide chemistry be identified, one that will allow the synthesis of highly membrane permeable analogs of Rp-cAMPS.

Initial attempts to overcome the limitations of Rp-cAMPS involved the introduction of 8-bromo (8-Br) or 8-(4-chlorophenylthio) (8-pCPT) substitutions on Rp-cAMPS to generate more lipophilic analogs such as Rp-8-Br-cAMPS and Rp-8-pCPT-cAMPS (6). However, these analogs were not optimal owing to their modest membrane permeability. Subsequently, it was thought that uncharged acetoxymethyl ester (AM-ester) prodrug derivatives of Rp-cAMPS might constitute a new class of cAMP antagonist with high membrane permeability. This expectation was based on the successful synthesis of AM-esters of cAMP and cGMP (7, 8). However, for the AM-ester of Rp-cAMPS, it soon became apparent that its use/application was complicated by an unexpected instability of the end product in which a significant amount of the agonist cAMP was generated spontaneously (Schultz C. and Schwede F., written communication).

We now report the synthesis of novel highly membrane permeable para-acetoxybenzyl (pAB) ester prodrug derivatives of Rp-cAMPS. These prodrugs include Rp-cAMPS-pAB, Rp-8-Br-cAMPS-pAB, and Rp-8-pCPT-cAMPS-pAB, each of which is quickly and efficiently bioactivated by cytosolic esterases that are ubiquitously expressed in mammalian cells. Importantly, we find that these prodrugs are useful tools for biological research, because they exhibit reasonable hydrolytic stability while also acting with micromolar or even nanomolar potency to disrupt cAMP signaling in living cells. The effectiveness of such pAB-based prodrugs as inhibitors of PKA activation is validated in assays of HEK cells expressing genetically encoded fluorescence resonance energy transfer (FRET) and bioluminescence resonance energy transfer (BRET) biosensors, or in a rat insulin 1 gene promoter (RIP1)-cAMP response element (CRE) luciferase assay (RIP1-CRE-Luc) that is specific for cAMP-stimulated gene expression.

Using perifusion assays of biphasic insulin secretion from isolated human and rat islets of Langerhans, we also report that the first-phase kinetic component of glucose-stimulated insulin secretion (GSIS) is nearly abrogated during treatment of islets with Rp-8-Br-cAMPS-pAB. This finding resolves a decades-old controversy first advanced by Charles et al (9) concerning whether or not glucose alone exerts cAMP-dependent actions to stimulate insulin secretion (9–20). Equally important, we find that Rp-8-Br-cAMPS-pAB antagonizes not only PKA activation, but also by the activation of cAMP-regulated guanine nucleotide exchange factors (GEFs) designated as Epac1 and Epac2 and that are encoded by the *RAPGEF3* and *RAPGEF4* genes, respectively. Thus, new findings presented here concerning human and rat islets encourage a reinterpretation of previously published reports in which Rp-cAMPS was used as a specific inhibitor of PKA-regulated insulin secretion.

Materials and Methods

High-performance liquid chromatography

Detailed methods for HPLC are presented in Supplemental Materials and Methods. All reagents were of analytical grade or HPLC grade available from commercial suppliers. Acetonitrile (CH_3CN) and dimethyl sulfoxide (DMSO) were stored over activated molecular sieves for at least 2 weeks before use. UV spectra were recorded with a Helios β-spectrometer (Spectronic Unicam). Mass spectra were obtained with an Esquire LC 6000 spectrometer (Bruker Daltronics) in the electrospray ionization mass spectrometry (ESI-MS) mode with 50% water/50% methanol as matrix. Nuclear magnetic resonance (NMR) spectra were recorded with a Varian Inova 500 MHz (Agilent) by Deutero with tetramethylsilane and 85% phosphoric acid as standards for ^{1}H and ^{31}P.

Synthesis of Rp-8-Br-cAMPS-pAB

Synthesis of 8-Br-cAMPS, Rp-isomer, 4-acetoxybenzyl ester (Rp-8-Br-cAMPS-pAB) was performed as described by Schwede et al (21) with some modifications. Rp-8-Br-cAMPS (50 μmol) and diisopropylethylammonium salt were suspended in 1000 μL dried CH_3CN in a 2-mL polypropylene reaction tube with screw cap. After addition of 250 μmol (38.3 μL, 5 eq.) 4-(chloromethyl)phenyl acetate and 50 μmol (8.56 μL, 1 eq.) of diisopropylethylamine, the reaction mixture was shaken in a MHL 20 thermomixer (HLC Biotech) set at 25°C and 400 rpm. Progress of pAB-ester formation was monitored by analytical HPLC with 45% CH_3CN as eluent. After completion of the reaction (18 h), volatile components were evaporated in a SpeedVac concentrator under reduced pressure with oil pump vacuum. The residue was suspended in 300 μL CH_3CN and was extracted with hexane (3 $\times$ 1.5 mL) to remove unreacted chloromethyl reagent. Purification was performed with preparative HPLC using 40% CH_3CN as eluent. Rp-8-Br-cAMPS-pAB (33.4 μmol) was obtained with a purity of 99.6% (by HPLC) (yield: 66.8%). Formula, $C_{19}H_{19}BrN_5O_7PS$ (MW: 572.3). See Supplemental Materials and Methods for ESI-MS and NMR values.

Synthesis of Rp-cAMPS-pAB

Synthesis of adenosine-cAMPS, Rp-isomer, 4-acetoxybenzyl ester (Rp-cAMPS-pAB) was performed in parallel reactions with 2×100 μmol of Rp-cAMPS, diisopropylethylammonium salt, as described for Rp-8-Br-cAMPS-pAB. The reaction was completed after 24 hours. Purification with preparative HPLC (35% CH_3CN) and workup as described above led to 39 μmol Rp-cAMPS-pAB (purity: 99.4% [by HPLC]; yield: 19.5%). Formula, $C_{19}H_{20}N_5O_7PS$ (MW: 493.4). See Supplemental Materials and Methods for ESI-MS and NMR values.

Synthesis of Rp-8-pCPT-cAMPS-pAB

Synthesis of 8-(4-chlorophenylthio)adenosine-cAMPS, Rp-isomer, 4-acetoxybenzyl ester (Rp-8-pCPT-cAMPS-pAB) was performed using Rp-8-pCPT-cAMPS (215 μmol), diisopropylethylammonium salt, 240 μmol (36.9 μL, 1.1 eq.) 4-(chloromethyl)phenyl acetate, 215 μmol (36.8 μL, 1 eq.) diisopropylethylamine, 2800 μL dried CH_3CN, and 200 μL dried DMSO were added to a 3.5-mL polypropylene reaction tube with screw cap. The reaction mixture was placed in a thermomixer (25°C/400 rpm) for 21 hours. Workup and purification (45% CH_3CN) of the crude reaction product was as described above for Rp-8-Br-cAMPS; 111.2 μmol Rp-8-pCPT-cAMPS-pAB was obtained with a purity of 99.3% (by HPLC) (yield: 51.7%). Formula, $C_{25}H_{23}ClN_5O_7PS_2$ (MW: 636.1). See Supplemental Materials and Methods for ESI-MS and NMR values.

Bioactivation of Rp-cAMPS-pAB esters

Homogenates of insulin-secreting cell lines were prepared as described in Supplemental Materials and Methods. Reaction conditions for analysis of Rp-cAMP-pAB ester bioactivation are described in Supplemental Materials and Methods. Methods concerning the use of HPLC for analysis of Rp-cAMPS-pAB ester bioactivation end products are in Supplemental Materials and Methods.

Cell culture

Normal HEK cells or HEK cells stably expressing the glucagon-like peptide-1 (GLP-1) receptor (GLP-1R) (HEK-GLP-1R cells) were from ATCC or Novo Nordisk A/S, respectively. HEK cells for BRET were from DSMZ (catalog no. ACC-305). HEK cell clones expressing A-kinase activity reporter 3 (AKAR3), Epac1, and Epac2 were generated by O.G. Chepurny (22, 23). DMEM with 25mM glucose was used for HEK cell culture. INS-1 cells (p78) from M. Asfari (Université Paris, France) were cultured in RPMI 1640 containing 11.1mM glucose (24). MIN6 cells (p29) provided by J. Miyazaki (Osaka University, Japan) were cultured in DMEM containing 25mM glucose (25). Cultures were passaged once a week while maintained at 37°C in a humidified incubator that was gassed with 5% CO_2. Culture media and additives were from Life Technologies.

Luciferase reporter assays

The luciferase assay using RIP1-CRE-Luc was performed as described previously (26). RIP1-CRE-Luc generated by O.G. Chepurny consists of 4 multimerized nonpalindromic CREs found within RIP1 and fused to the coding sequence of firefly luciferase in pLuc-MCS (26). Transient transfections with this plasmid were performed using Lipofectamine and Plus reagent according to the manufacturer's protocol (Life Technologies). For experiments, cells were exposed for 4 hours to serum-free medium containing 0.1% BSA and test substances. Cells were lysed in Passive Lysis buffer (Promega), and lysates were assayed in triplicate for photoemissions using a luciferase assay kit (Promega) and a FlexStation 3 microplate reader (Molecular Devices). Experiments were performed 48 hours after transfection.

FRET reporter assays

HEK cell clones stably expressing AKAR3, Epac1, and Epac2 FRET reporters (22, 23) were plated at 80% confluence on 96-well clear bottom assay plates (Costar 3904) coated with rat tail collagen (RTC) (Collaborative Biomedical Products). HEK-GLP-1R cells (27) transduced for 16 hours with AKAR3 virus (28) were cultured at a density of approximately 60 000 cells/well under conditions in which the multiplicity of infection was equivalent to 25 viral particles per cell. The culture media was removed and replaced by 170 μL/well of a standard extracellular saline solution containing 11mM glucose and 0.1% BSA so that assays of FRET could be performed using a FlexStation 3 microplate reader (22, 23). Excitation light was delivered at 435/9 nm (455 nm cut-off), and emitted light was detected at 485/15 nm (cyan fluorescent protein) or 535/15 nm (yellow fluorescent protein). The emission intensities were the average of 12 excitation flashes for each time point per well. Test solutions dissolved in standard extracellular saline containing 0.1% DMSO were placed in V-bottom 96-well plates (Greiner Bio-One) and an automated pipetting procedure was used to transfer 30 μL of each test solution to the assay plate containing cells. The cyan fluorescent protein to yellow fluorescent protein emission ratio was calculated for each well, and the values for 8 wells were averaged. The time course of the change of FRET ratio was plotted after exporting data to Origin 8.0 (OriginLab).

BRET reporter assays

BRET assays used HEK cells cotransfected with a PKA regulatory subunit Rluc8 construct (hRIα or hRIIα) and a GFP^2-hCα catalytic subunit construct. This approach allows for the expression of recombinant PKA holoenzymes with known subunit composition (29, 30). Transfection of HEK cells was achieved using polyethyleneimine-coated microspheres (6μM, 24 kDa, linear) from Polysciences, Inc. Transfected cells were seeded on white 96-well Nunc plates (Thermo Scientific), and BRET assays were performed 48 hours after transfection. On the day of the assay, the HEK cells expressing recombinant PKA holoenzymes were rinsed twice with Dulbecco's PBS (DPBS), after which they were treated for 20 minutes with DPBS containing the indicated test substances. The solution was then replaced with DPBS containing the same test substances plus a luciferase substrate (coelenterazine 400A, 5μM; BIOTREND Chemikalien). After an additional 15-minute incubation, the BRET emission ratio was determined using a POLARstar Omega microplate reader (BMG Labtech).

Rap1 activation assays

Epac-catalyzed Rap1 GTPase activation was monitored in vitro using purified recombinant full-length (FL) Epac1 (human) and Epac2 (mouse) proteins in combination with purified C-terminal truncated Rap1b(1–167). These proteins were expressed in *Escherichia coli* and purified, as described previously (31). Epac1 or Epac2 GEF activity was monitored in vitro using

Rap1b(1–167) preloaded with a fluorescent guanosine 5′-diphosphate (GDP) analog of BODIPY (boron-dipyrromethene) from Life Technologies; catalog no. G-22360). Rap1b(1–167) loaded with BODIPY-GDP was then incubated with Epac1 or Epac2 in a buffer containing excess free GDP. BODIPY-GDP dissociates from Rap1b(1–167) and is replaced by GDP when the GEF activity of Epac1 or Epac2 is activated by cAMP, and this dissociation is monitored as a decrease of BODIPY-GDP fluorescence (32). The assay was performed using 500nM Rap1b(1–167) BODIPY GDP and 200nM Epac1 or Epac2 dissolved in 50mM Tris-HCl (pH 7.5), 50mM NaCl, 5mM $MgCl_2$, 1mM dithiothreitol, and 50μM GDP and the indicated concentrations of Rp-cAMPS analogs at room temperature using half-area 96-well plates (Corning Costar). A control vehicle solution or 25μM cAMP dissolved in the vehicle solution was used to monitor dissociation of BODIPY-GDP from Rap1b(1–167) under baseline conditions or cAMP-stimulated conditions, respectively. The exchange reaction was monitored using a Spectramax M2 Plate Reader (Molecular Devices) with the excitation and emission wavelengths set at 485 and 515 nm, respectively.

Rat islet insulin secretion assays

Sprague-Dawley rats fed a standard chow (TekLad Diet 2014; Harlan Laboratories) were housed in an Association for Assessment and Accreditation of Laboratory Animal Care-accredited facility at Lilly Research Laboratories. For 12-week-old male rats, the pancreas was surgically removed under conditions of isofluorane anesthesia followed by cervical dislocation, as stipulated in an animal use protocol approved by the Eli Lilly Institutional Animal Care and Use Committee. After inflation of the pancreas with a Hank's balanced salt solution (Life Technologies, catalog no. 14175–103) containing collagenase (VitaCyte, LCC, catalog no. 005–1030), the pancreas was subjected to collagenase digestion (14 min) to obtain islets. These islets were cultured overnight in RPMI 1640 medium containing 11.1mM glucose, 10% fetal bovine serum (FBS), glutamine (2mM GlutaMax; Life Technologies), and penicillin-streptomycin. Perifusion assays of secreted insulin were performed the next day, as described previously (33). Briefly, 50 islets were immobilized on a P-4 gel matrix (Bio-Gel, Bio-Rad Laboratories) within perifusion chambers housed in a 37°C climate-controlled enclosure (Biorep Perifusion System). For each chamber, a peristaltic pump delivered HEPES-buffered saline solution containing: 120mM NaCl, 4.8mM KCl, 2.5mM $CaCl_2$, 1.2mM $MgCl_2$, 10mM HEPES, 24mM $NaHCO_3$, and 0.25% BSA at a flow rate of 100 μL/min. Perifusates were collected at 4°C using a robotic fraction collector (BioRep) designed for 96-well plates. Insulin content in the perifusates was quantified by electrochemical luminescence detection using an MSD insulin assay kit (Meso Scale Discovery, catalog no. K152BZC). The amount of secreted insulin was normalized relative to islet DNA content for each chamber, as determined using a MagMax-96 DNA assay kit (Life Technologies).

Human islet insulin secretion assays

Human islets were isolated from pancreata of 7 healthy anonymous organ donors (age: 53.1 ± 4.3 y; body mass index: 29.7 ± 2.1; 72% female) at the Alberta Diabetes Institute IsletCore or the Clinical Islet Laboratory at the University of Alberta. The islets were cultured overnight in low-glucose (5.5mM) DMEM with L-glutamine, 110 mg/L sodium pyruvate, 10% FBS, and 100 U/mL penicillin/streptomycin. All studies were approved by the Human Research Ethics Board (Pro00001754) at the University of Alberta. All organ donors provided informed consent for use of pancreatic tissue in medical research. Perifusion assays of secreted insulin were performed as described above for rat islets except that experiments were performed 2–3 days after isolation.

Statistical analyses

The repeatability of findings was confirmed by performing each experiment a minimum of 2 times. FRET, luciferase, and INS-1 cell insulin secretion assay data were evaluated for statistical significance by Student's paired *t* test (Systat Software, Inc). Analysis of BRET data was performed using Tukey's test and GraphPad Prism software. For studies of islet insulin secretion, statistical significance was evaluated using an ANOVA test follow by a Dunnett's correction (rat islets), or a Bonferroni post hoc test (human islets). For all assays, $P < .05$ was considered to be statistically significant.

Sources of reagents

cAMP analogs (for a complete list with abbreviations, see Supplemental Materials and Methods) were from the BIOLOG Life Science Institute. Forskolin, 3-isobutyl-1-methylxanthine (IBMX), exendin-4 (Ex-4), and 4-acetoxybenzyl alcohol (pAB) were from Sigma-Aldrich.

Results

Synthesis and metabolism of pAB prodrug derivatives of Rp-cAMPS

pAB derivatives of Rp-cAMPS were synthesized using a reaction scheme (Supplemental Figure 1) analogous to that first described for the synthesis of cAMP-AM and cGMP-AM esters (7, 8, 21). Based on theoretical considerations (34, 35), rapid bioactivation of Rp-cAMPS-based pAB derivatives is initiated with the hydrolysis of the terminal acyl group by cytosolic esterases, followed by spontaneous 1,4-elimination and hydrolysis in order to generate 4-hydroxybenzyl alcohol and the unesterified Rp-cAMPS analogs that act intracellularly as cAMP antagonists (Supplemental Figure 2A). However, it is also possible that these pAB derivatives of Rp-cAMPS will undergo nucleophilic attack at the central phosphorous atom in order to generate sulfur-free cAMP analogs that will act as agonists in assays of PKA activation (Supplemental Figure 2B). To determine which of these 2 possible routes of conversion is of physiological relevance, we examined bioactivation of Rp-8-pCPT-cAMPS-pAB in lysates of rat INS-1 cells, a cell line commonly used in studies of cAMP-regulated insulin secretion (24). INS-1 cell lysates were spiked with Rp-8-pCPT-cAMPS-pAB and incubated at 37°C for 15 minutes, after which HPLC analysis demonstrated that esterase-catalyzed hydrolysis

of Rp-8-pCPT-cAMPS-pAB predominated so that Rp-8-pCPT-cAMPS was the principal metabolite detected (Supplemental Figure 3). Notably, the rate of bioactivated hydrolytic conversion under these conditions was fast ($t_{1/2}$ of 3–4 min) and stoichiometric (~99% efficiency), not only for INS-1 cell lysates but also for lysates of mouse MIN6 insulin-secreting cells (25) or human serum (Table 1). Nearly identical findings were obtained using Rp-8-Br-cAMPS-pAB and Rp-cAMPS-pAB (Table 1). Thus, pAB derivatization is a suitable means by which to generate cAMP antagonists that are highly membrane permeable prodrugs and that undergo fast bioactivation intracellularly.

Bioactivation of Rp-8-Br-cAMPS-pAB by cytosolic esterases

Only trace amounts of the PKA activator 8-Br-cAMP appeared in the INS-1 cell lysates after incubation of Rp-8-Br-cAMPS-pAB at 37°C (Table 1). Thus, the ratio of hydrolytically released Rp-8-Br-cAMPS to 8-Br-cAMP was approximately 99:1. When INS-1 cell lysates were denatured by heat to inactivate cytosolic esterases (99°C, 60 min), the rate of hydrolytic conversion of Rp-8-Br-cAMPS-pAB was dramatically reduced ($t_{1/2}$ of 87 min), and the ratio of released Rp-8-Br-cAMPS to 8-Br-cAMP was approximately 1:1.5 (Table 1). However, for phosphate or Tris-buffered solutions not containing cell lysates, the spontaneous chemical hydrolysis of Rp-8-Br-cAMPS-pAB was slow ($t_{1/2}$ of 114 min), and the ratio of released Rp-cAMPS to 8-Br-cAMP was approximately 1:15 (Table 1). This suggests that spontaneous hydrolysis favors the slow formation of cAMP analogs not containing the Rp moiety, whereas rapid esterase-mediated hydrolysis preserves the Rp moiety. Thus, the effectiveness of pAB compounds depends on the level of intracellular esterase activity.

Rp-8-Br-cAMPS-pAB inhibits AKAR3 activation by cAMP-elevating agents

In a side-by-side comparison of cAMP analogs with or without pAB derivatization, the potency of Rp-8-Br-cAMPS-pAB as a cAMP antagonist was determined to be greatly enhanced. This was established in a spectrofluorimetric assay of HEK cell clone C12 that expresses the genetically encoded biosensor AKAR3 (22, 23). AKAR3 is an A-kinase activity reporter that exhibits an increase of FRET (ΔFRET) measurable as a decrease of the 485/535 nm emission ratio when it is phosphorylated by PKA (36). For the analysis presented here, C12 monolayers were grown in a 96-well format, and measurements of FRET were obtained while performing automated injection of test solutions into individual wells. Using this approach, AKAR3 accurately reports cAMP-dependent activation of PKA, as validated using the PKA activator 6-Bn-cAMP-AM in combination with the Ser/Thr protein kinase inhibitor H-89 (30).

Our analysis of clone C12 demonstrated no ΔFRET in response to Rp-8-Br-cAMPS-pAB alone, whereas this analog exerted a dose-dependent action to antagonize the ΔFRET induced by cAMP-elevating agents forskolin and IBMX (cf, Figure 1, A and B). This antagonism was mediated by the Rp-8-Br-cAMPS moiety of Rp-8-Br-cAMPS-pAB, because no such antagonism was measured when C12 cells were instead treated with 10μM 4-acetoxybenzyl alcohol (designated here as pAB) serving as a negative control reagent for the prodrug group (Figure 1C). Remarkably, we found that 3.0μM Rp-8-Br-cAMPS-pAB fully blocked the actions of forskolin (2μM) and IBMX (100μM) at AKAR3 (Figure 1B). In contrast, 300μM non-pAB analog Rp-8-Br-cAMPS was ineffective, acting only to slow the rate of AKAR3 activation, while failing to prevent full activation (Figure 1D). These findings demonstrated that the pAB substitution on Rp-

Table 1. Analysis of pAB-Based cAMPS Analog Bioactivation Properties

Incubation medium	Rp-8-Br-cAMPS-pAB $t_{1/2}$ (min)	Rp-cAMPS-pAB $t_{1/2}$ (min)	Rp-8-pCPT-cAMPS-pAB $t_{1/2}$ (min)	Released analog ratio
INS-1 homogenate[a]	3	4	2	~99:1
MIN6 homogenate[a]	4	6	3	~99:1
20% human serum, 80% 50mM PBS; pH 7.4	2	3	4	~99:1
10% FBS, 90% 50mM PBS; pH 7.4	37	49[b]	196[c]	~2:1 to ~1:3
50mM PBS; pH 7.4	114	124[b]	273[c]	~1:15 to ~1:25
50mM Tris/HCl; pH 7.4	114	114[b]	217[c]	~1:5 to ~1:15
Heat-inactivated INS-1 homogenate (99°C, 60 min)	87	n.d.	n.d.	~1:1.5

[a] Lysis buffer for preparation of homogenates contained 50mM Tris/HCl, 200mM NaCl, and 10mM dithiothreitol; pH 7.4.

[b] Buffer contained 5% CH_3CN to avoid precipitation during prolonged incubations.

[c] Buffer contained 25% CH_3CN to avoid precipitation during prolonged incubations.

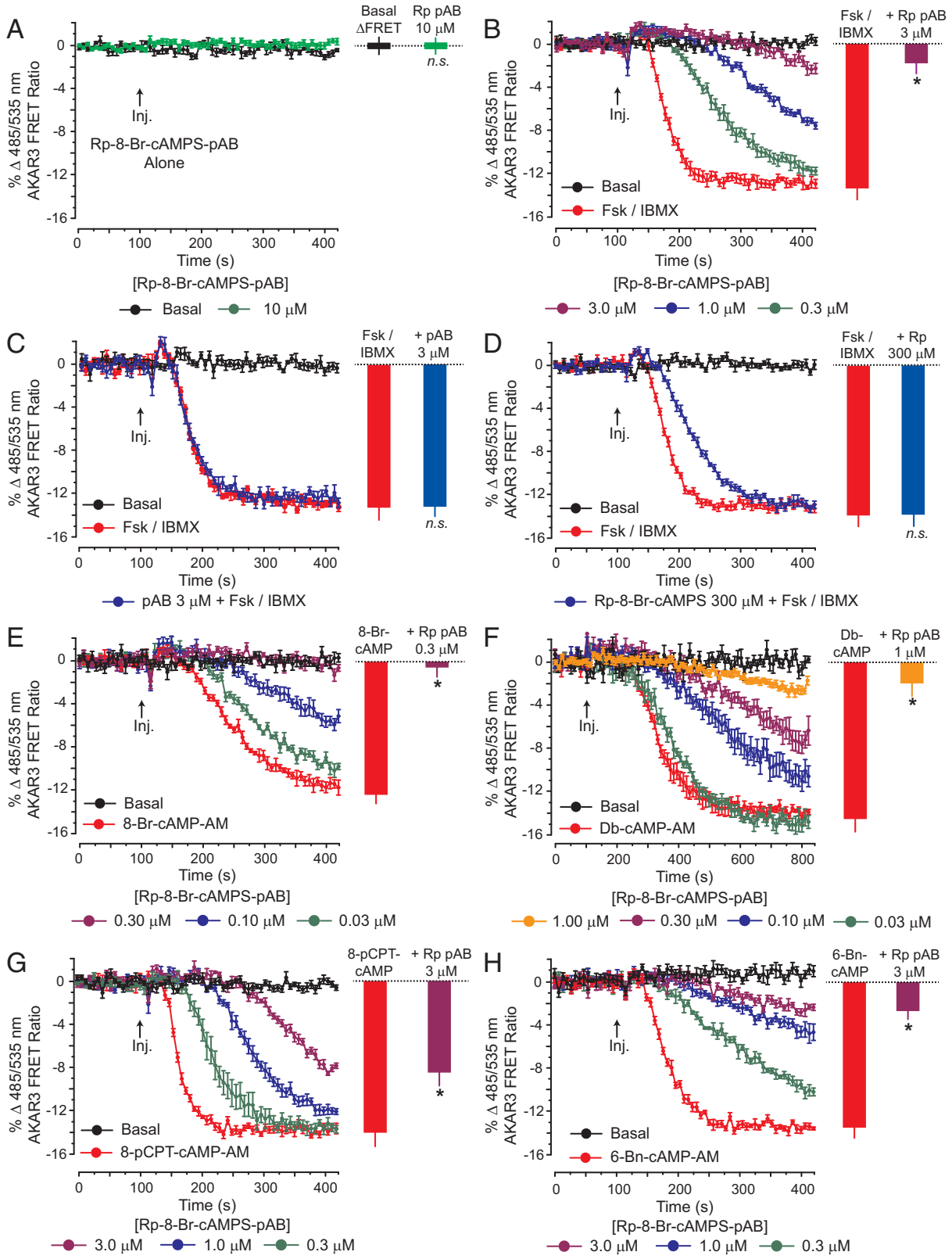

Figure 1. Rp-8-Br-cAMPS-pAB blocks AKAR3 activation. A, The AKAR3 to FRET ratio in HEK C12 cells was unaffected by simple injection (Inj.) of Rp-8-Br-cAMPS-pAB alone. B, Combined administration of forskolin (Fsk) (2μM) and IBMX (100μM) produced a decrease of AKAR3 FRET ratio (ΔFRET), and this was antagonized by Rp-8-Br-cAMPS-pAB. C, The ΔFRET measured in response to Fsk and IBMX was not antagonized by pAB alone. D, The non-pAB analog Rp-8-Br-cAMPS failed to block the end-point ΔFRET measured in response to Fsk and IBMX but did slow the initial rate of change of FRET when tested at 300μM, which is 100 times the maximum efficacious concentration of Rp-8-Br-cAMPS-pAB. E–H, Rp-8-Br-

8-Br-cAMPS afforded increased antagonist potency as a consequence of increased membrane permeability.

Rp-8-Br-cAMPS-pAB was also a potent antagonist of AKAR3 activation induced by 10μM each of 8-Br-cAMP-AM, Db-cAMP-AM, 8-pCPT-cAMP-AM, and 6-Bn-cAMP-AM (Figure 1, E–H). Most notably, 0.3μM Rp-8-Br-cAMP-pAB fully blocked the stimulatory action of 10μM 8-Br-cAMP-AM at AKAR3 (Figure 1E). Thus, pAB derivatization afforded nanomolar inhibitory potency in these assays of AKAR3 activation. However, it should be emphasized that cytosolic esterase-catalyzed hydrolysis of Rp-8-Br-cAMPS-pAB will generate bioactive Rp-8-Br-cAMPS that accumulates intracellularly in a time-dependent manner (34). For this reason, the intracellular concentration of bioactive Rp-8-Br-cAMPS is potentially in the micromolar range or higher. Despite this trapping effect, the utility of pAB derivatization chemistry is illustrated by the fact that an increased antagonist potency was also achieved for the analogs Rp-8-pCPT-cAMPS-pAB and Rp-cAMPS-pAB (Figure 2, A–D).

FRET assays were also performed using HEK-GLP-1R cells (27) that stably express the human GLP-1R and that were transduced with an adenovirus (28) that directs the expression of AKAR3. In assays using the GLP-1R agonist Ex-4 (a cAMP-elevating agent) (37, 38), AKAR3 was activated in a dose-dependent manner using concentrations of Ex-4 as low as 10pM (Figure 2E). As expected, this action of Ex-4 was reduced by the PKA inhibitor H-89 and also by Rp-8-Br-cAMPS-pAB when each was tested at 10μM (Figure 2, F and G). However, 300μM Rp-8-Br-cAMPS was ineffective as an antagonist of AKAR3 activation (Figure 2H). Such findings establish that pAB derivatization of Rp-8-Br-cAMPS is a highly effective strategy by which to generate a cAMP antagonist that blocks G protein-coupled receptor signal transduction.

Figure 1 (Continued). cAMPS-pAB also antagonized AKAR3 activation induced by 10μM each of 8-Br-cAMP-AM (E), Db-cAMP-AM (F), 8-pCPT-cAMP-AM (G), and 6-Bn-cAMP-AM (H) in HEK C12 cells. For Db-cAMP-AM, the x-axis scaling is extended from 0 to 800 seconds to account for the slower onset of the ΔFRET in response to this analog. The slower action of Db-cAMP-AM is explained by the fact that released Db-cAMP must undergo additional intracellular metabolism in order to hydrolytically remove the butyryl moiety at the 2′-position on the ribose ring so that it can activate PKA. For B–H, HEK cells were pretreated for 15 minutes with cAMP antagonists or the pAB control at the indicated final concentrations. The injected test solutions containing Fsk, IBMX, or cAMP agonists also contained cAMP antagonists or the pAB control at the indicated final concentrations. Each FRET ratio data point indicates the mean $\pm$ SD of n = 12 wells. Histogram plots provide statistical comparisons for n = 3 experiments. *, $P < .05$, *t* test. n.s., not significant.

pAB derivatives of Rp-cAMPS inhibit cAMP-stimulated gene expression

We next sought to determine whether pAB derivatives of Rp-cAMPS exert long-term actions to inhibit cAMP signaling and gene expression. To this end, HEK cells were transfected with RIP1-CRE-Luc (26), a reporter that is a sensitive read-out for gene expression stimulated by cAMP-elevating agents. The CRE of RIP1-CRE-Luc binds CREB (cAMP response element-binding protein), and CREB is phosphorylated by PKA in order to stimulate luciferase (Luc) gene expression. RIP1-CRE-Luc was first developed by Chepurny in studies of RIP1, and it contains 4 nonpalindromic CREs found within RIP1 (26). The synthetic RIP1-CRE-Luc reporter is especially well suited for assays of gene expression, because it has low basal activity and wide dynamic range (26). Our analysis revealed that Rp-8-Br-cAMPS-pAB dose dependently inhibited the actions of forskolin (2μM) and IBMX (100μM) to stimulate RIP1-CRE-Luc activity in transfected HEK cells (Figure 3A).

When HEK cells were pretreated with various cAMP antagonists for 30 minutes, after which there was a 4-hour coadministration of these antagonists with both forskolin and IBMX, it was possible to demonstrate that the antagonist action of Rp-8-Br-cAMPS-pAB was approximately 100-fold more potent than that of the non-pAB analog Rp-8-Br-cAMPS (cf, Figure 3, A and B). We then determined that the parent analog Rp-cAMPS was ineffective in this assay, whereas Rp-cAMPS-pAB exerted a dose-dependent inhibitory effect (cf, Figure 3, C and D). Notably, Rp-8-Br-cAMPS-pAB also blocked the action of GLP-1R agonist Ex-4 to stimulate RIP1-CRE-Luc activity in HEK-GLP-1R cells, whereas Rp-8-Br-cAMPS was ineffective (cf, Figure 3, E and F). Independent confirmation of these findings concerning PKA-regulated gene expression was obtained in assays of Ser-133 CREB phosphorylation status using HEK cell lysates. PKA-dependent CREB phosphorylation stimulated by forskolin and IBMX was inhibited by Rp-8-Br-cAMPS-pAB, whereas Rp-8-Br-cAMPS was ineffective (Supplemental Figure 4).

PKA holoenzyme dissociation is antagonized by Rp-8-Br-cAMPS-pAB

To validate that pAB derivatives of Rp-cAMPS antagonize cAMP-dependent dissociation of PKA, we performed BRET assays of HEK cells expressing recombinant PKA holoenzymes that have defined subunit composition. For this purpose, Rluc8 luciferase was fused to the C terminus of RI or RII PKA regulatory subunit isoforms (29, 30). These regulatory subunit constructs were then cotransfected with a GFP^2-hCα construct in which a human PKA catalytic subunit (Cα) was fused to a

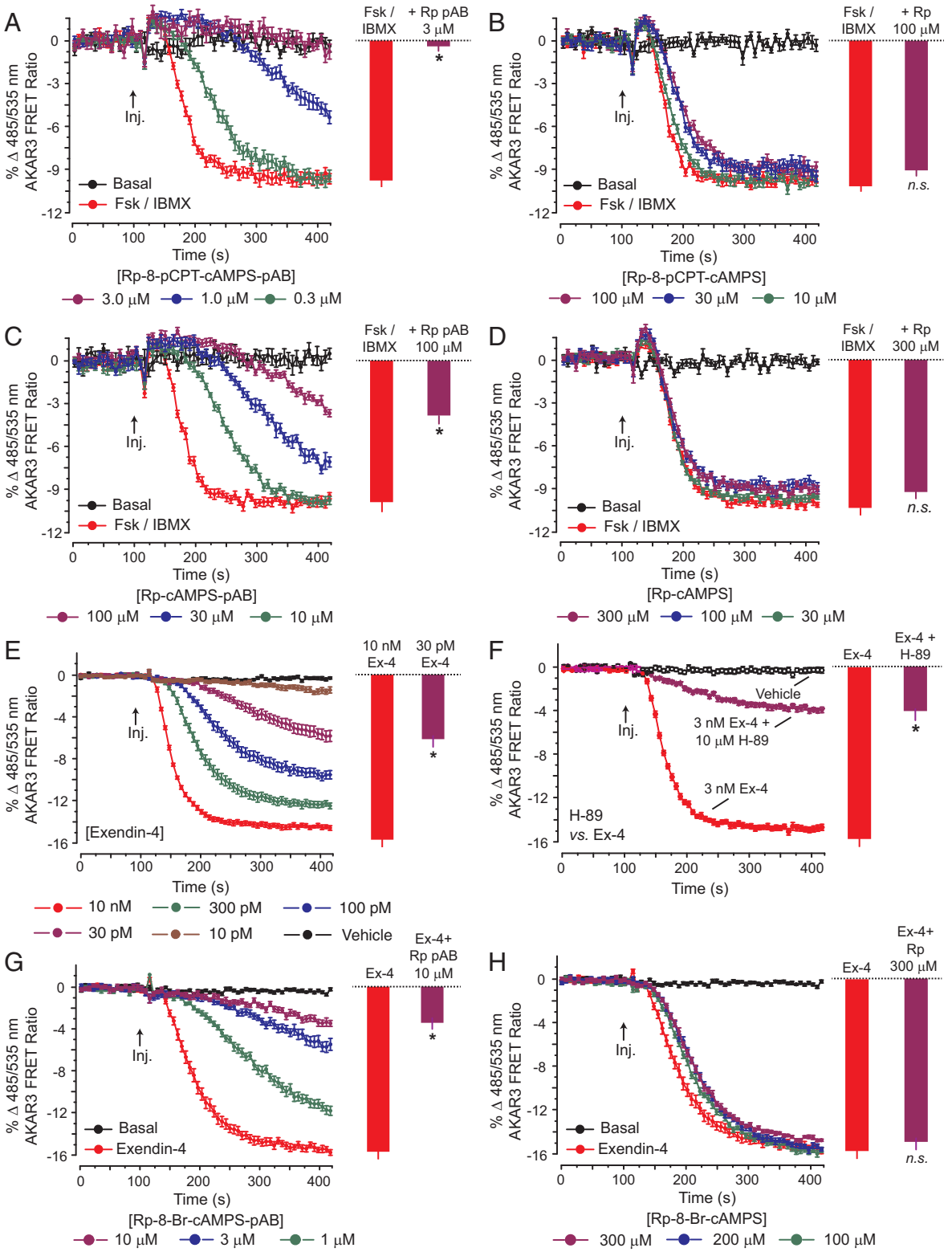

Figure 2. Additional cAMP antagonists for signal transduction research. A and B, Differential properties of Rp-8-pCPT-cAMPS-pAB (A) and Rp-8-pCPT-cAMPS (B) in the AKAR3 activation assay (95) using HEK C12 cells treated with forskolin (Fsk) (2μM) and IBMX (100μM). C and D, Differential actions of Rp-cAMPS-pAB (C) and Rp-cAMPS (D). E, Dose-dependent activation of AKAR3 by GLP-1R agonist exendin-4 (Ex-4). F and G, Validation that PKA inhibitor H-89 (10μM) and cAMP antagonist Rp-8-Br-cAMPS-pAB (1μM–10μM) reduce the action of Ex-4 (3nM) to activate AKAR3 in HEK-GLP-1R cells. H, Failure of Rp-8-Br-cAMPS (100μM–300μM) to block AKAR3 activation by Ex-4 (3nM) in HEK-GLP-1R cells. Each FRET ratio data point indicates the mean ± SD of n = 12 wells. Histogram plots provide statistical comparisons for n = 3 experiments. *, $P < .05$, *t* test.

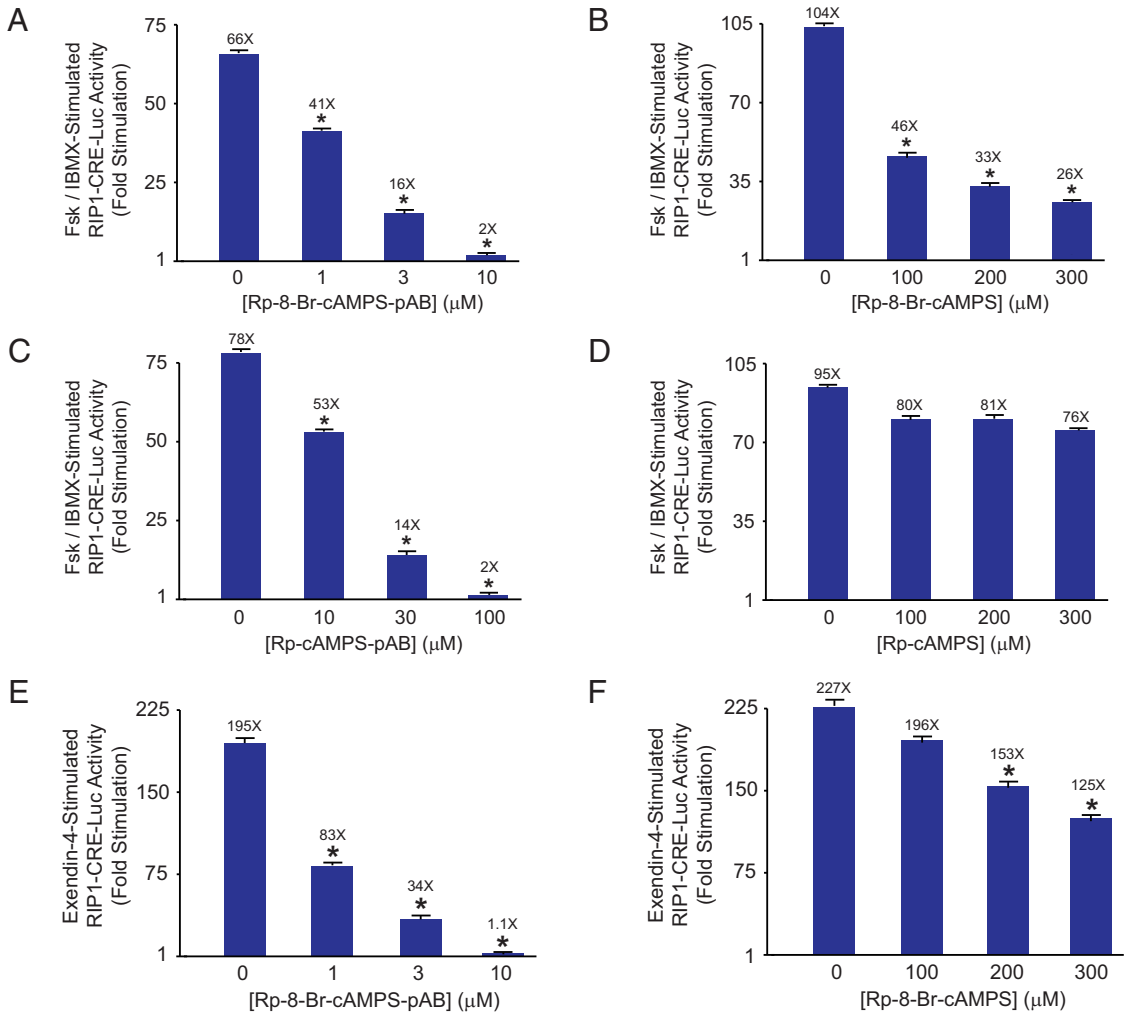

Figure 3. Rp-8-Br-cAMPS-pAB and Rp-cAMPS-pAB inhibit RIP1-CRE-Luc activity. A and B, Low concentrations of Rp-8-Br-cAMPS-pAB antagonized the actions of forskolin (Fsk) (2μM) and IBMX (100μM) to activate RIP1-CRE-Luc in transfected HEK cells (A), whereas higher concentrations of Rp-8-Br-cAMPS were less effective (B). C and D, Rp-cAMPS-pAB effectively inhibited RIP1-CRE-Luc activation (C), whereas Rp-cAMPS did not (D). E and F, Differential antagonist properties of Rp-8-Br-cAMPS-pAB and Rp-8-Br-cAMPS to inhibit the action of GLP-1R agonist Ex-4 (10nM) to stimulate RIP1-CRE-Luc gene expression in HEK-GLP-1R cells. For A–F, histogram plots provide statistical comparisons for n = 3 experiments for each analog tested. *, $P < .05$, *t* test. Error bars indicate mean ± SD.

variant of green fluorescent protein (GFP^2) (29, 30). In this assay, reconstitution of the recombinant PKA holoenzymes occurred in HEK cells, and BRET was measured as intermolecular energy transfer between Rluc8 and GFP^2. When levels of cytosolic cAMP rise, the resultant activation of PKA is accompanied by holoenzyme dissociation and a decrease of BRET (29, 30).

When the cAMP-elevating agents forskolin and IBMX were added to individual wells of a 96-well plate, PKA holoenzyme dissociation was measurable as a decrease of the GFP^2 to Rluc8 BRET emission ratio monitored at 515 nm (GFP^2) and 410 nm (Rluc8). For PKA holoenzymes containing the RIα (Figure 4, A and B) or RIIα (Figure 4, C and D) regulatory subunit isoforms, the decrease of BRET in response to forskolin and IBMX was fully blocked by 10μM Rp-8-Br-cAMPS-pAB (Figure 4, A and C). However, 10μM non-pAB analog Rp-8-Br-cAMPS was only marginally effective as an antagonist (Figure 4, B and D). In fact, the concentration of Rp-8-Br-cAMPS had to be increased to 1mM in order to block RIα regulatory subunit-mediated holoenzyme dissociation (Figure 4B). In contrast, RIIα-mediated holoenzyme dissociation remained relatively resistant to 1mM Rp-8-Br-cAMPS (Figure 4D). These findings are consistent with the earlier report that Rp-8-Br-cAMPS is a more selective antagonist at the PKA holoenzyme comprised of RIα regulatory subunits (6).

Inhibition of Epac1 and Epac2 activation by Rp-8-Br-cAMPS-pAB

Rp-8-Br-cAMPS-pAB was also evaluated for its potential ability to antagonize the activation of cAMP-regu-

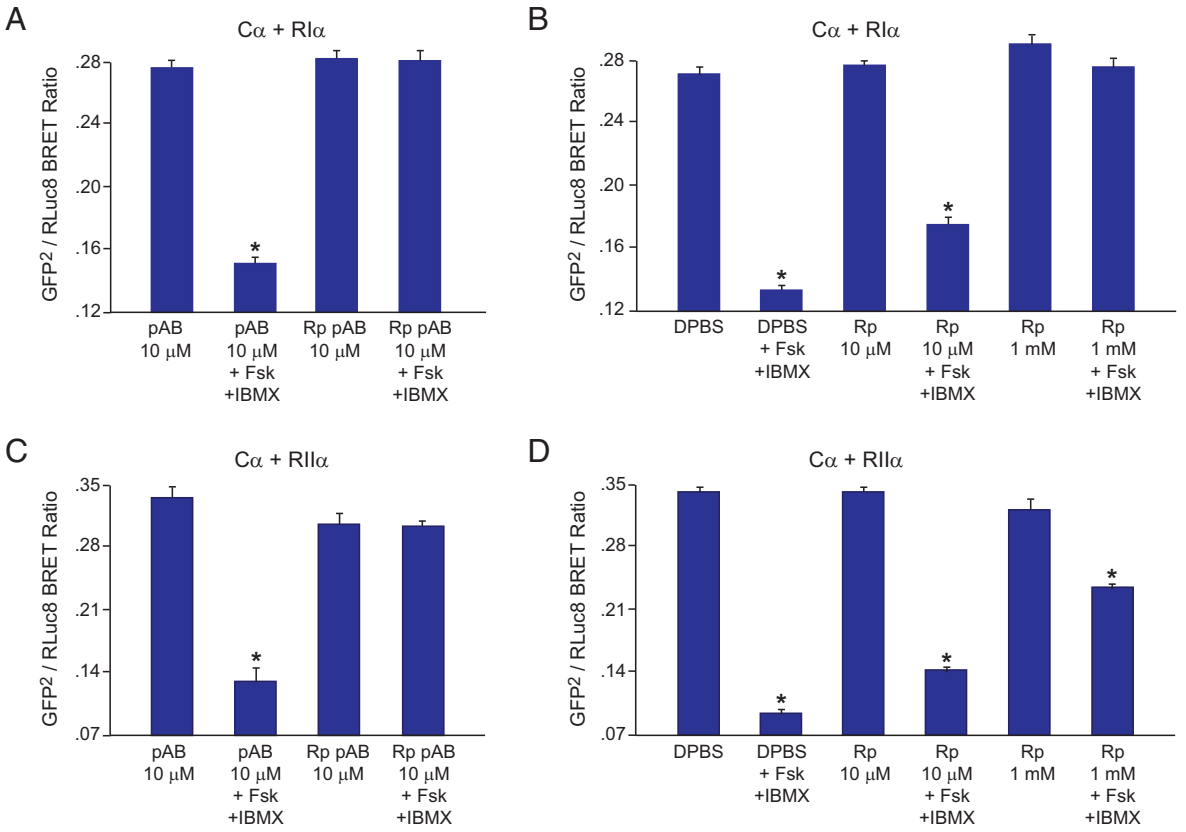

Figure 4. Rp-8-Br-cAMPS-pAB antagonizes PKA holoenzyme activation. A–D, BRET assays of PKA subunit interaction in HEK cells coexpressing a GFP^2-hCα PKA catalytic subunit and either the type Iα (A and B) or type IIα (C and D) PKA regulatory subunit isoforms fused to Rluc8. A decrease of BRET ratio signifies PKA holoenzyme dissociation in response to binding of cAMP to PKA regulatory subunits under conditions in which cells are equilibrated in DPBS. Forskolin (Fsk) (50μM) and IBMX (100μM) fully stimulated PKA holoenzyme dissociation (A–D), and the accompanying decrease of BRET ratio was fully antagonized by Rp-8-Br-cAMPS-pAB (Rp pAB) (10μM) coadministered with Fsk and IBMX (A and C). Rp-8-Br-cAMPS (Rp) (10μM) was less effective as an antagonist (B and D). When the Rp-8-Br-cAMPS concentration was raised to 1mM, full antagonism of RIα-mediated holoenzyme dissociation was measurable (B), whereas RIIα-mediated holoenzyme dissociation was not fully blocked (D). Histogram plots provide statistical comparisons for a single representative experiment. *, $P < .05$, Tukey's test. Each BRET ratio is the mean ± SEM of n = 6 wells.

lated GEFs Epac1 and Epac2 (39, 40). To this end, FRET reporters that incorporate FL Epac1 and Epac2 were used to generate the HEK cell clones C9 and C1, respectively (22, 23). Unlike AKAR3, the FL Epac1 and Epac2 FRET reporters exhibit a decrease of FRET in response to cAMP, and this ΔFRET is measurable as an increase of the 485/535 nm FRET ratio (22, 23). To activate the FL Epac1 and Epac2 FRET reporters, we used 8-pCPT-2′-*O*-Me-cAMP-AM, a highly membrane permeable AM-ester of an Epac-selective cAMP analog (ESCA-AM), also known as 007-AM (41–44).

When the ESCA-AM was applied to C9 or C1 cells expressing the FL Epac1 and Epac2 FRET reporters, a rapid increase of the 485/535 nm FRET ratio was measured (Figure 5, A and B). This ΔFRET is consistent with a rapid bioactivation of the ESCA-AM so that free 8-pCPT-2′-*O*-Me-cAMP can bind to the reporters (41, 42). When C9 and C1 cells were instead pretreated for 15 minutes with Rp-8-Br-cAMPS-pAB, it dose dependently inhibited the ability of the ESCA-AM to stimulate a ΔFRET (Figure 5, A and B). However, no such inhibition was measured when cells were pretreated with 10μM negative control pAB compound (data not shown). Thus, preliminary evidence was provided that intracellularly bioactivated Rp-8-Br-cAMPS-pAB has the capacity to antagonize Epac1 and Epac2 activation by 8-pCPT-2′-*O*-Me-cAMP.

To obtain independent confirmation of these findings, we performed in vitro Rap1 activation assays using Epac1, Epac2, and Rap1b(1–167). In these assays using purified and recombinant proteins, the binding of cAMP to Epac1 or Epac2 allows the GEF activity of Epac to catalyze fluorescent BODIPY-GDP exchange on Rap1b(1–167), thereby generating a decrease of BODIPY-GDP fluorescence (32). It was established that cAMP-stimulated and Epac1-mediated activation of Rap1b(1–167) was antagonized by Rp-cAMPS (as reported by Rehmann et al [45]), and also by Rp-8-Br-cAMPS (Figure 6, A and B). We then obtained the novel finding that these analogs blocked Rap1b(1–167) activation mediated by Epac2 (Figure 6, C and D). Interestingly, for Epac1, we found that Rp-8-Br-cAMPS alone had a weak

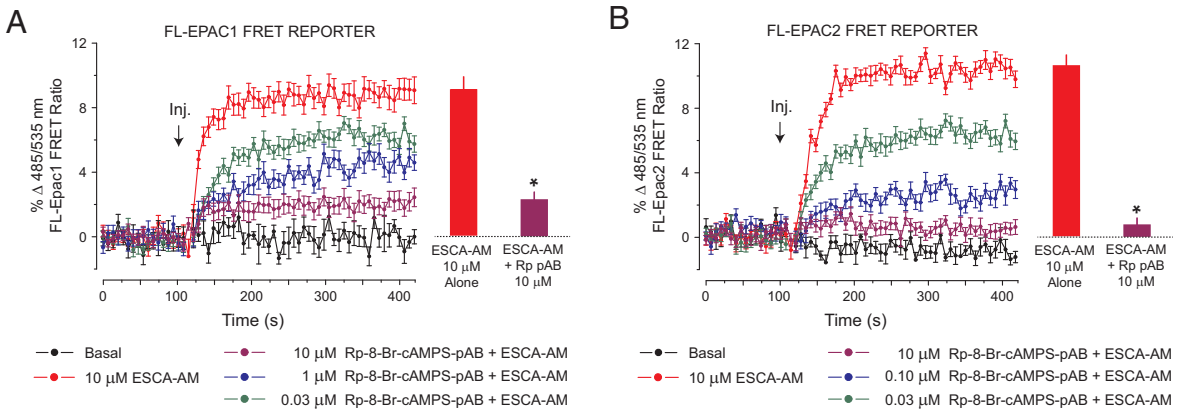

Figure 5. Rp-8-Br-cAMPS-pAB antagonizes Epac FRET reporter activation. A and B, HEK cell clones C9 and C1 expressing FL Epac1 (A) and Epac2 (B) FRET reporters exhibited an increase of 485/535 nm emission ratio signifying a decrease of FRET measured in response to the Epac activator 8-pCPT-2′-*O*-Me-cAMP-AM (ESCA-AM). Note that a 15-minute pretreatment of C9 or C1 cells with increasing concentrations of Rp-8-Br-cAMPS-pAB dose dependently inhibited the ΔFRET measured in response to the ESCA-AM. Each FRET ratio data point indicates the mean ± SD of n = 12 wells. Histogram plots provide statistical comparisons for n = 3 experiments. *, $P < .05$, *t* test. Rp pAB, Rp-8-Br-cAMPS-pAB.

stimulatory effect before the addition of cAMP (Figure 6B, arrow). However, this was not the case for Epac2 (Figure 6D). Collectively, these findings indicate that the pAB conjugates of Rp-cAMPS can be used not only as inhibitors of PKA activation but also as inhibitors of Epac1 and Epac2 activation. Such findings have important implications for the interpretation of previous studies using Rp-cAMPS analogs.

Rp-8-Br-cAMPS-pAB inhibits GSIS

cAMP exerts PKA and Epac mediated actions to stimulate insulin release from pancreatic β-cells (2, 3, 28, 46–

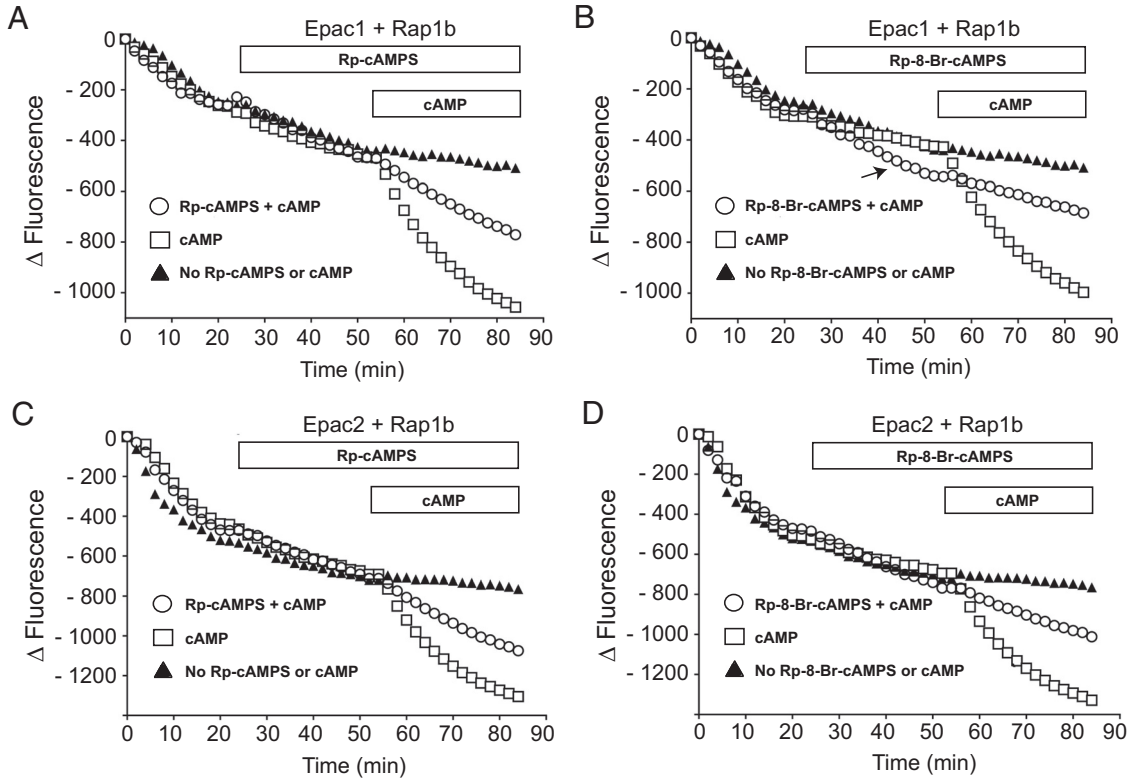

Figure 6. Rp-cAMPS-based analogs inhibit in vitro Rap1 activation. A and B, Rap1 activation assays using purified recombinant human (rh) Epac1 and Rap1b(1–167). Note that 200μM Rp-cAMPS (A) or Rp-8-Br-cAMPS (B) blocked Rap1b(1–167) activation by 25μM cAMP. Also note that Rp-8-Br-cAMPS alone exerted a weak stimulatory effect before the addition of cAMP (arrow in B). C and D, Rap1(1–167) activation assays using purified recombinant mouse Epac2 and Rap1b(1–167) and performed as described for A and B. Horizontal bars at the top indicate exposure intervals. Y-axes in A–D indicate arbitrary units of light intensity for calibration of the change of fluorescence (Δ fluorescence). Each experiment was repeated a total of 3 times with similar results.

58). However, assessment of how cAMP exerts its effect is hampered by the poor membrane permeability of available pharmacological agents (59). To evaluate a potential usefulness of Rp-8-Br-cAMPS-pAB for studies of insulin secretion, pilot assays were performed using the rat insulinoma cell line INS-1. These assays demonstrated that Rp-8-Br-cAMPS-pAB inhibited the actions of glucose, forskolin, and IBMX to stimulate insulin secretion, whereas Rp-8-Br-cAMPS was ineffective (Supplemental Figure 5A). As expected, the expression of multiple PKA regulatory subunit isoforms in INS-1 cells was validated (Supplemental Figure 5B), and it was also possible to use a Kemptide phosphorylation assay to demonstrate that extracellularly administered Rp-8-Br-cAMPS-pAB inhibited PKA activation in response to Db-cAMP-AM and 6-Bnz-cAMP-AM (Supplemental Figure 5, C and D).

Although INS-1 cells are a convenient model system for in vitro assays, they have a limited usefulness due to the fact that they are not fully differentiated but are instead transformed cells with properties not completely identical to authentic β-cells (24). As an alternative to INS-1 cells, we performed perifusion assays of insulin secretion from rat islets so that it could be determined whether Rp-8-Br-cAMPS-pAB altered first- and/or second-phase GSIS (20). It is known that rat islets are especially well-suited for the study of biphasic GSIS, because they typically generate a fast transient first-phase increase of insulin secretion that is easily distinguished from second-phase GSIS when using methods of rapid perifusion (60–62). Our primary goal was to evaluate the potential role of cAMP as a permissive factor, or a coupling factor, linking β-cell glucose metabolism to insulin secretion. This concept has remained controversial for over 40 years (9–20, 28, 48, 49, 58).

When rat islets were perifused with buffer not containing Rp-8-Br-cAMPS-pAB, first- and second-phase GSIS was stimulated by a step-wise increase of the glucose concentration from 2.8mM to 16.7mM (Figure 7A). Under these conditions, first-phase GSIS was nearly abrogated when rat islets were treated with 10μM Rp-8-Br-cAMPS-

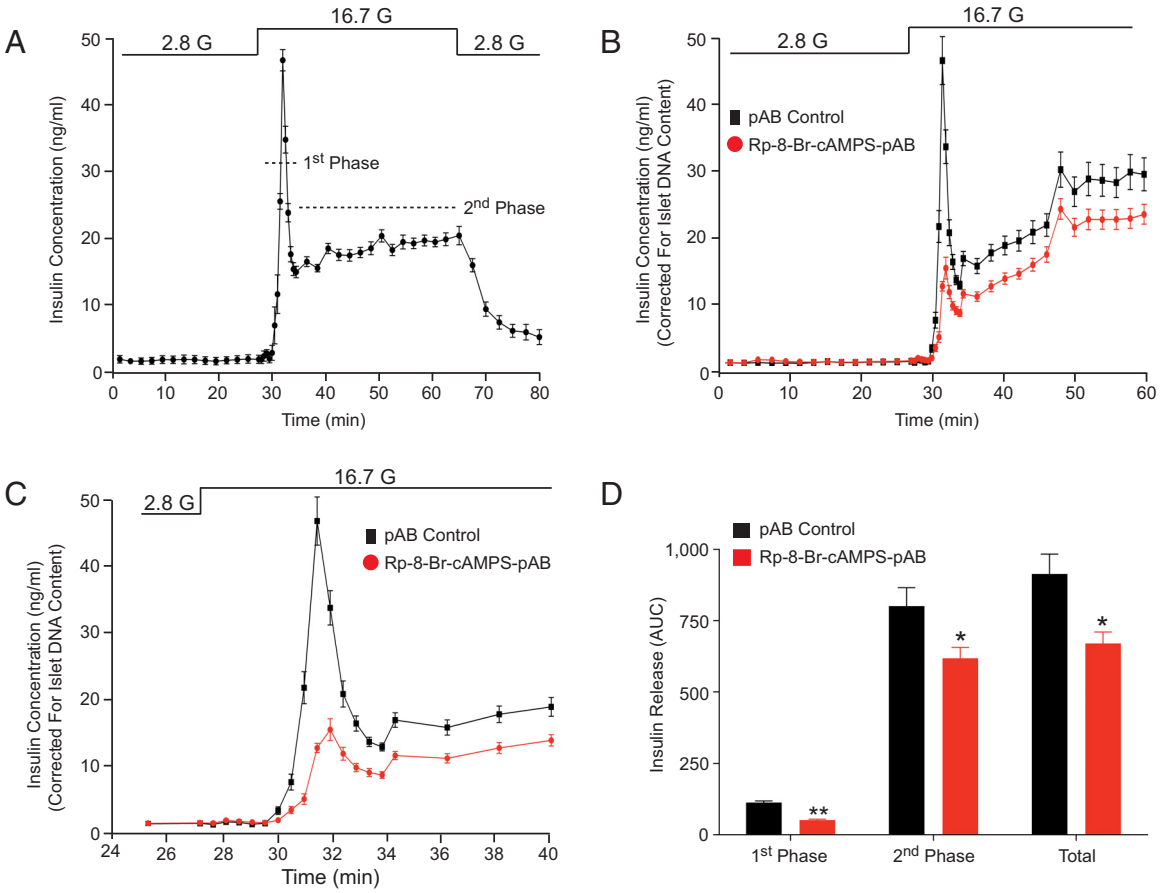

Figure 7. Rp-8-Br-cAMPS-pAB inhibits GSIS from rat islets. A, A step-wise increase of the islet perifusate glucose concentration from 2.8mM to 16.7mM elicited biphasic insulin secretion. B, Rp-8-Br-cAMPS-pAB (10μM) suppressed GSIS, whereas the negative control pAB compound (10μM) did not. C, Expansion of B demonstrates that first-phase GSIS was nearly abrogated under conditions of perifusion with Rp-8-Br-cAMPS-pAB. D, An area-under-the-curve (AUC) analysis for B summarizes the action of Rp-8-Br-cAMPS-pAB to inhibit GSIS. Each histogram bar indicates the mean ± SEM for n = 6 perifusion chambers per experimental treatment. Statistical significance (*, $P < .05$; **, $P < .001$) was evaluated using ANOVA followed by a Dunnett's correction. Similar findings were obtained in 2 additional experiments. G, glucose.

pAB (Figure 7, B and C). Surprisingly, the amplitude of second-phase GSIS was only modestly reduced (Figure 7B), and basal insulin secretion was unaffected (Supplemental Figure 6A). Importantly, the inhibitory action of the Rp-8-Br-cAMPS-pAB prodrug was mediated by cytosolic esterase-catalyzed generation of Rp-8-Br-cAMPS, because first-phase GSIS was retained under conditions in which islets were instead perifused with 10μM pAB compound serving as a negative control (Figure 7, B and C). These findings are summarized in a histogram plot that quantifies insulin secretion using an area-under-the-curve analysis for first- and second-phase GSIS (Figure 7D).

Finally, we evaluated whether Rp-8-Br-cAMPS-pAB inhibited GSIS from human islets (Figure 8). In these assays of n = 7 donor islet preparations, basal insulin secretion was monitored by perifusion of islets with buffer containing 2.8mM glucose, whereas stimulated insulin secretion was evoked by 11.1mM glucose. Pooling of the data demonstrated that 10μM Rp-8-Br-cAMPS-pAB inhibited first-phase GSIS, whereas second-phase GSIS was not significantly altered (Figure 8A). This action of Rp-8-Br-cAMPS-pAB is illustrated on an expanded time scale that emphasizes insulin secretion corresponding to first-phase GSIS (Figure 8B). For the individual donor islet

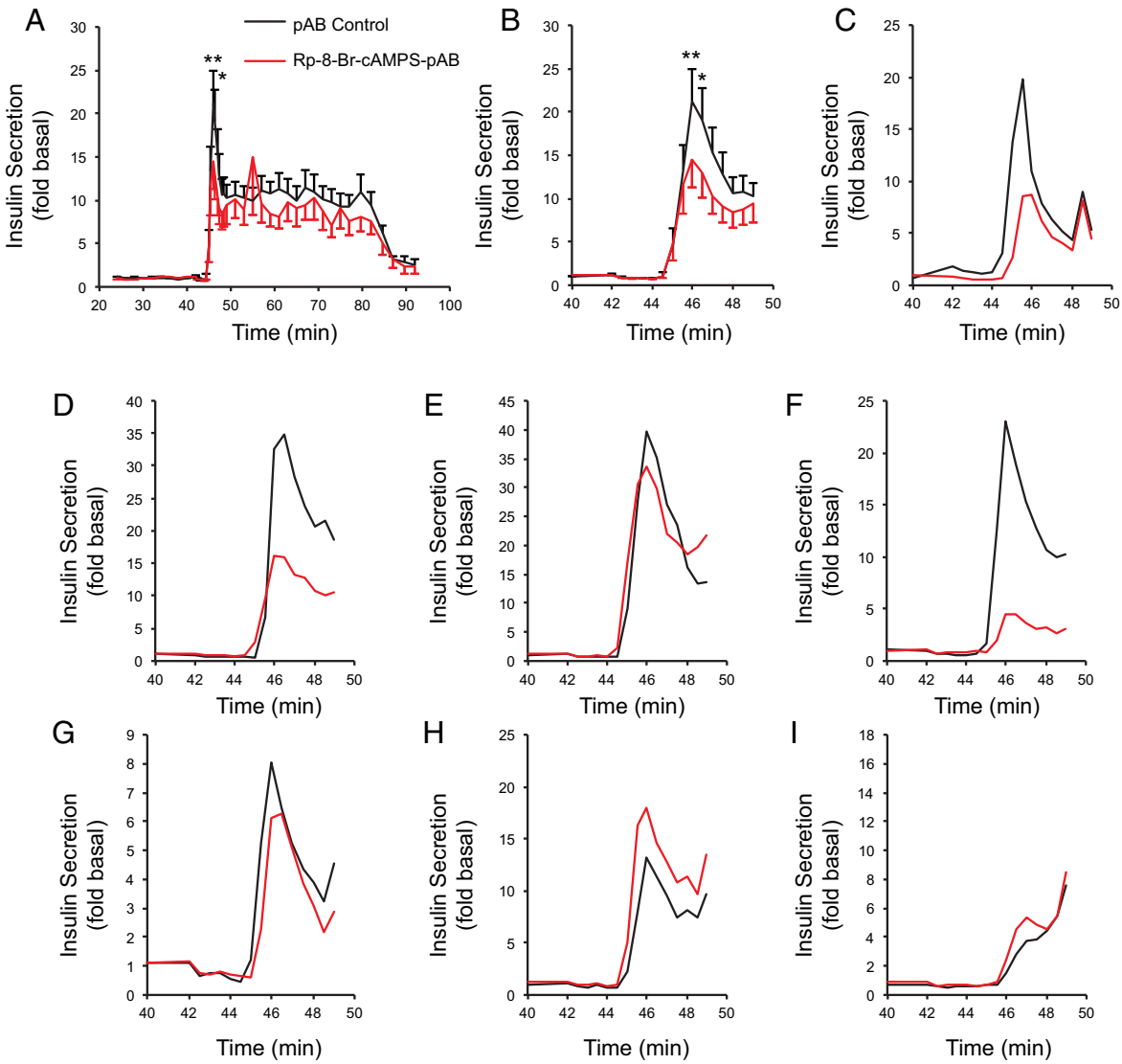

Figure 8. Rp-8-Br-cAMPS-pAB inhibits GSIS from human islets. A–I, Insulin secretion stimulated by 11.1mM glucose is shown as the fold increase from basal levels at 2.8mM. A and B, Pooled data from 6 islet preparations, in which first-phase GSIS was measurable. C–I, Insulin secretion profiles from islets of individual donors. The islets of the single donor in I were excluded from the analysis in A and B due to the lack of first-phase GSIS. Interassay variability is expected in view of the fact that human islets are prone to postmortem ischemia that can occur during surgical removal of the pancreas. Variability may also be explained by genetic factors that influence first-phase GSIS (96–98). For A and B, data are the mean ± SEM fold increase of insulin secretion on compressed (A) or expanded (B) time scales. For C–I, each secretion profile is the average obtained from 2 perifusion lanes of islets (15 islets/chamber). Basal secretion at 2.8mM glucose at the 30-minute time point was 727 ± 140 pg/mL (A); 11.1mM glucose was applied at the 42-minute time point and was switched back to 2.8mM at the 77-minute time point. Two-way repeated measures ANOVA followed by a Bonferroni post hoc test (*, $P < .05$; **, $P < .01$).

preparations, examples of the insulin secretion profiles are provided in Figure 8, C–I. Because a single islet preparation exhibited no first-phase GSIS (Figure 8I), this preparation was excluded from the analysis presented in Figure 8, A and B. Importantly, Rp-8-Br-cAMPS-pAB failed to alter basal insulin secretion that was measured under conditions in which the perifusate contained 2.8mM glucose (Supplemental Figure 6B).

Discussion

New evidence for cAMP-dependent actions of glucose to stimulate insulin secretion

Over 40 years ago, it was reported that glucose metabolism raises levels of cAMP in isolated islets (9–20). Charles et al (9) also reported that for rat islets, the time course of glucose-stimulated cAMP production matched that of first-phase GSIS. At that time, speculation existed concerning a possible role for cAMP as a permissive factor or a coupling factor linking glucose metabolism to insulin secretion. However, these findings were largely ignored in later years because the ability of glucose to stimulate cAMP production was small, whereas a stronger effect was measured in response to cAMP-elevating agents such as forskolin. Then, in 1990, Persaud et al (63) reported that rat islet GSIS was not blocked by Rp-cAMPS. Subsequently, Sato and Henquin investigated the newly discovered "amplification" pathway of GSIS, and it too was found to be unaffected by Rp-cAMPS (64). When assessing these earlier findings concerning Rp-cAMPS, it is important to note that this analog has low membrane permeability (1). However, prolonged exposure of islets to a high concentration of Rp-cAMPS was reported to block the action of forskolin to potentiate GSIS, whereas it failed to influence the action of glucose alone (63, 64). Harris et al (65) also reported that for rat islets, the secretagogue action of glucose was unaffected by small myristoylated synthetic peptides that are membrane permeable and that are derived from the larger endogenous protein kinase A inhibitor peptide. Similarly, Lester et al (66) reported that rat islet GSIS was unaffected by synthetic peptides that disrupt the interaction of PKA regulatory subunits with A-kinase anchoring proteins. Importantly, all such studies with rat islets were performed using methods of static incubation, in which there was insufficient temporal resolution to detect first-phase GSIS.

We now report that rapid perifusion techniques reveal a capacity of Rp-8-Br-cAMPS-pAB to nearly abrogate first-phase GSIS from human and rat islets. This fast component of GSIS is initiated by a "triggering" pathway of β-cell stimulus-secretion coupling in which depolarization-induced Ca^{2+} influx stimulates the exocytosis of a readily-releasable pool of secretory granules (67–69). Based on findings presented here, glucose-stimulated cAMP production might lead to PKA activation with resultant phosphorylation of SNARE (soluble NSF attachment protein receptor) complex-associated proteins such as Snapin that facilitate exocytosis of the readily-releasable pool (52). Simultaneously, cAMP may act via Epac proteins to promote Rap1 activation with consequent activation of a novel phospholipase Cϵ that links cAMP production to β-cell Ca^{2+} influx, Ca^{2+} mobilization, and protein kinase C activation (50, 51, 70–72).

When considering how glucose raises levels of cAMP in β-cells, Kasai and coworkers originally proposed that glucose metabolism provides substrate ATP for adenylyl cyclase-catalyzed cAMP production, PKA activation, and insulin exocytosis (48, 49, 56). Tengholm (53) and Tengholm and coworkers (73–77) more recently reported that compartmentalized cAMP production at the plasma membrane allows glucose metabolism to raise levels of cAMP, thereby promoting insulin secretion. The exact biochemical mechanisms linking glucose metabolism to cAMP production remain debated because competing evidence exists for roles of transmembrane adenylyl cyclases (48, 49, 56, 73–82) and soluble adenylyl cyclase (adenylyl cyclase 10; AC-10) (58, 83). Potentially, glucose metabolism generates CO_2 that is converted by carbonic anhydrase to bicarbonate ion, which then activates soluble adenylyl cyclase to stimulate cAMP production (58, 83). Interestingly, metabolic compensation of β-cells under conditions of diet-induced obesity leads to a situation in which Epac2 plays an increasingly important role in GSIS, possibly by promoting the exocytosis of "restless newcomer" secretory granules (84–87).

New pAB-based prodrugs for cyclic nucleotide research

Here, we also address a fundamental limitation of present-day cyclic nucleotide research, in which the analysis of cAMP signaling is impeded by the lack of suitable cAMP antagonists that act with high potency when they are administered extracellularly. Although (Rp)-phosphorothioates of cAMP such as Rp-cAMPS are commonly used as selective cAMP antagonists, their effectiveness for studies of living cells is compromised due to their low lipophilicity and poor membrane permeability (1). Using a pAB conjugation chemistry first reported by Jessen et al (35) in studies of nucleoside diphosphates, we report that pAB-ester prodrug derivatives of Rp-cAMPS act quickly to block PKA activation. Potentially, this pAB conjugation chemistry can be applied to other small mol-

ecules to achieve highly efficient prodrug delivery intracellularly.

Because intracellular metabolism of Rp-8-Br-cAMPS-pAB by cytosolic esterases will generate 4-acetoxybenzyl alcohol in addition to bioactive Rp-8-Br-cAMPS, future studies of other cell types should evaluate whether 4-acetoxybenzyl alcohol is inert, toxic, or bioactive on its own. For the assays reported here, no such secondary effects are apparent, because we find that exposure of islets to 4-acetoxybenzyl alcohol fails to alter basal levels of insulin secretion, nor does it disrupt GSIS. Furthermore, exposure of HEK cells to 4-acetoxybenzyl alcohol fails to disrupt CRE-dependent gene transcription. However, potential off-target effects of 4-acetoxybenzyl alcohol in other cell types need to be determined because such effects might be cell type specific. The high potency of Rp-8-Br-cAMPS-pAB favors the use of low concentrations of this antagonist, thereby minimizing any toxic effects. Indeed, we find that in assays of AKAR3 activity, the antagonist action of Rp-8-Br-cAMPS-pAB is evident using concentrations as low as 30nM (Figure 1E).

Conclusion

An interesting outgrowth of the present study is the demonstration that Rp-cAMPS and its related analog Rp-8-Br-cAMPS have the capacity to partially antagonize the cAMP-dependent activation of Rap1 in an in vitro Rap1 activation assay that uses Epac1 or Epac2 as the cAMP-binding partners (Figure 6). Furthermore, Rp-8-Br-cAMPS weakly activates Epac1, as reported previously (88). Collectively, these findings reinforce the concept that analogs of Rp-cAMPS exert mixed agonist/antagonist actions at Epac proteins (89). Furthermore, it is clear that the pAB derivatives of Rp-cAMPS reported here should also be considered to be broad-spectrum antagonists of PKA, Epac1, and Epac2 activation. Such findings have important implications for the interpretation of previous findings in which Rp-cAMPS was used as a specific antagonist of PKA activation. For example, intracellularly administered Rp-cAMPS was used in previous patch clamp studies of mouse islets to differentiate between PKA-dependent and PKA-independent actions of cAMP to stimulate insulin exocytosis (3, 49, 90). Using human islets, a permissive role for PKA in support of GSIS was also explored through the use of Rp-8-pCPT-cAMPS (28). Because we find that Rp-cAMPS antagonizes Epac1 and Epac2 activation, it could be that previous studies underestimated a role for Epac proteins as determinants of insulin secretion. Intriguingly, there is known to exist a characteristic loss of first-phase GSIS in early stages of human type 2 diabetes mellitus (91–93). In these patients, first-phase GSIS can be restored rapidly upon administration of the cAMP-elevating hormone GLP-1 (38, 94). The challenge now is to relate these clinical findings concerning type 2 diabetes mellitus to a possible dysfunction of glucose-stimulated cAMP production and cAMP signaling in pancreatic β-cells.

Acknowledgments

We thank Irmtraud Hammerl-Witzel and Natascha Mumdy (University of Kassel) for assistance in the preparation of cell cultures for BRET assays; J.S. Bos and H. Rehmann (University Utrecht) for providing Epac1, Epac2, and Rap1b(1–167) plasmids; State University of New York Upstate student Parisa Afshari for pilot assays concerning Rp-8-Br-cAMPS-pAB; the Human Organ Procurement and Exchange program and the Trillium Gift of Life Network for their efforts in obtaining human organs for research; and Dr James Shapiro and Dr Tatsuya Kin at the Clinical Islet Laboratory (University of Alberta) and Dr James Lyon from the Alberta Diabetes Institute IsletCore for human islet isolations.

Author contributions: F.S. and H.-G. G. performed synthesis, purification, and metabolism of cyclic nucleotides; O.G.C. and C.A.L. conducted FRET, Luc, CREB, Kemptide, and INS-1 insulin secretion assays. M.K., D.B., and F.W.H. conducted BRET and PKA immunoblot assays; O.C. conducted rat islet insulin secretion assays. J.E.M.F. and P.E.M. conducted human islet insulin secretion assays; Y.Z., F.M., and X.C. conducted Rap1 activation assays; M.K., D.B., F.W.H., C.A.L., O.C., and X.C. edited the manuscript; G.G.H., F.S., and O.G.C. wrote the manuscript; and G.G.H. organized the project.

Address all correspondence and requests for reprints to: George G. Holz, PhD, Professor of Medicine and Pharmacology, State University of New York Upstate Medical University, IHP 4310 at 505 Irving Avenue, Syracuse, NY 13210. E-mail: holzg@upstate.edu.

This work was supported by the National Institutes of Health Grant R01-DK069575 (to G.G.H.) and by American Diabetes Association Awards 7–12-BS-077 (to G.G.H.) and 1–12-BS-109 (to C.A.L.). F.W.H. was supported by the European Union FP7 Health Programme Contract 241481 (AFFINOMICS) and the Federal Ministry of Education and Research Grant FKZ 0316177F (No Pain). X.C. was supported by the National Institutes of Health Grant R01-GM066170. P.E.M. was supported by a grant-in-aid from the Canadian Diabetes Association (OG-3–14-4565-PM). Human islet isolations were funded in part by the Alberta Diabetes Foundation.

Disclosure Summary: O.G.C., M.K., D.B., C.A.L., O.C., Y.Z., F.M., X.C., J.E.M.F., P.E.M., F.W.H., and G.G.H. have nothing to disclose. F.S. and H.-G.G. are employed by the BIOLOG Life Science Institute that sells cAMP analogs that were used in this study.

References

1. **Schwede F, Maronde E, Genieser H, Jastorff B.** Cyclic nucleotide analogs as biochemical tools and prospective drugs. *Pharmacol Ther*. 2000;87(2–3):199–226.
2. **Renström E, Eliasson L, Rorsman P.** Protein kinase A-dependent and -independent stimulation of exocytosis by cAMP in mouse pancreatic B-cells. *J Physiol*. 1997;502(pt 1):105–118.
3. **Eliasson L, Ma X, Renström E, et al.** SUR1 regulates PKA-independent cAMP-induced granule priming in mouse pancreatic B-cells. *J Gen Physiol*. 2003;121(3):181–197.
4. **Takuma T, Ichida T.** Cyclic AMP antagonist Rp-cAMPS inhibits amylase exocytosis from saponin-permeabilized parotid acini. *J Biochem*. 1991;110(2):292–294.
5. **Branham MT, Mayorga LS, Tomes CN.** Calcium-induced acrosomal exocytosis requires cAMP acting through a protein kinase A-independent, Epac-mediated pathway. *J Biol Chem*. 2006; 281(13):8656–8666.
6. **Gjertsen BT, Mellgren G, Otten A, et al.** Novel (Rp)-cAMPS analogs as tools for inhibition of cAMP-kinase in cell culture. Basal cAMP-kinase activity modulates interleukin-1 β action. *J Biol Chem*. 1995;270(35):20599–20607.
7. **Schultz C, Vajanaphanich M, Harootunian AT, Sammak PJ, Barrett KE, Tsien RY.** Acetoxymethyl esters of phosphates, enhancement of the permeability and potency of cAMP. *J Biol Chem*. 1993;268(9):6316–6322.
8. **Zhuo M, Hu Y, Schultz C, Kandel ER, Hawkins RD.** Role of guanylyl cyclase and cGMP-dependent protein kinase in long-term potentiation. *Nature*. 1994;368(6472):635–639.
9. **Charles MA, Fanska R, Schmid FG, Forsham PH, Grodsky GM.** Adenosine 3′,5′-monophosphate in pancreatic islets: glucose-induced insulin release. *Science*. 1973;179(4073):569–571.
10. **Grill V, Cerasi E.** Activation by glucose of adenyl cyclase in pancreatic islets of the rat. *FEBS Lett*. 1973;33(3):311–314.
11. **Grill V, Cerasi E.** Stimulation by D-glucose of cyclic adenosine 3′:5′-monophosphate accumulation and insulin release in isolated pancreatic islets of the rat. *J Biol Chem*. 1974;249:4196–4201.
12. **Hellman B, Idahl LA, Lernmark A, Täljedal IB.** The pancreatic β-cell recognition of insulin secretagogues: does cyclic AMP mediate the effect of glucose? *Proc Natl Acad Sci USA*. 1974;71(9): 3405–3409.
13. **Grill V, Cerasi E.** Glucose-induced cyclic AMP accumulation in rat islets of Langerhans: preferential effect of the α anomer. *FEBS Lett*. 1975;54:80–83.
14. **Grill V, Asplund K, Hellerström C, Cerasi E.** Decreased cyclic AMP and insulin response to glucose in isolated islets of neonatal rats. *Diabetes*. 1975;24:746–752.
15. **Suzuki S, Oka H, Yasuda H, Yamashita K, Kaneko T, Oda T.** Effect of glucose on adenosine 3′,5′-monophosphate levels in rat pancreatic islets. *Endocrinol Jpn*. 1975;22:479–482.
16. **Zawalich WS, Karl RC, Ferrendelli JA, Matschinsky F.** M. Factors governing glucose induced elevation of cyclic 3′5′ AMP levels in pancreatic islets. *Diabetologia*. 1975;11:231–235.
17. **Charles MA, Lawecki J, Pictet R, Grodsky GM.** Insulin secretion. Interrelationships of glucose, cyclic adenosine 3:5-monophosphate, and calcium. *J Biol Chem*. 1975;250:6134–6140.
18. **Grill V, Cerasi E.** Enhancement by D_2O of glucose-induced cyclic AMP accumulation in rat islets of Langerhans. *FEBS Lett*. 1976; 68:165–169.
19. **Rabinovitch A, Grill V, Renold AE, Cerasi E.** Insulin release and cyclic AMP accumulation in response to glucose in pancreatic islets of fed and starved rats. *J Clin Invest*. 1976;58:1209–1216.
20. **Tsumura Y, Kobayashi K, Yoshida K, Kagawa S, Matsuoka A.** Dynamics of insulin and cyclic adenosine 3′,5′-monophosphate release from the perifused rat islets of Langerhans under a slow-rise stimulation with D-glucose and its anomers. *Endocrinol Jpn*. 1979; 26:245–253.
21. **Schwede F, Brustugun OT, Zorn-Kruppa M, Døskeland SO, Jastorff B.** Membrane-permeant, bioactivatable analogues of cGMP as inducers of cell death in IPC-81 leukemia cells. *Bioorg Med Chem Lett*. 2000;10:571–573.
22. **Tsalkova T, Mei FC, Li S, et al.** Isoform-specific antagonists of exchange proteins directly activated by cAMP. *Proc Natl Acad Sci USA*. 2012;109(45):18613–18168.
23. **Chen H, Tsalkova T, Chepurny OG, et al.** Identification and characterization of small molecules as potent and specific EPAC2 antagonists. *J Med Chem*. 2013;56(3):952–962.
24. **Asfari M, Janjic D, Meda P, Li G, Halban PA, Wollheim CB.** Establishment of 2-mercaptoethanol-dependent differentiated insulin-secreting cell lines. *Endocrinology*. 1992;130(1):167–178.
25. **Miyazaki J, Araki K, Yamato E, et al.** Establishment of a pancreatic β cell line that retains glucose-inducible insulin secretion: special reference to expression of glucose transporter isoforms. *Endocrinology*. 1990;127(1):126–132.
26. **Chepurny OG, Holz GG.** A novel cyclic adenosine monophosphate responsive luciferase reporter incorporating a nonpalindromic cyclic adenosine monophosphate response element provides optimal performance for use in G protein coupled receptor drug discovery efforts. *J Biomol Screen*. 2007;12(5):740–746.
27. **Gromada J, Rorsman P, Dissing S, Wulff BS.** Stimulation of cloned human glucagon-like peptide 1 receptor expressed in HEK 293 cells induces cAMP-dependent activation of calcium-induced calcium release. *FEBS Lett*. 1995;373(2):182–186.
28. **Chepurny OG, Kelley GG, Dzhura I, et al.** PKA-dependent potentiation of glucose-stimulated insulin secretion by Epac activator 8-pCPT-2′-O-Me-cAMP-AM in human islets of Langerhans. *Am J Physiol Endocrinol Metab*. 2010;298(3):E622–E633.
29. **Prinz A, Diskar M, Erlbruch A, Herberg FW.** Novel, isotype-specific sensors for protein kinase A subunit interaction based on bioluminescence resonance energy transfer (BRET). *Cell Signal*. 2006; 18(10):1616–1625.
30. **Chepurny OG, Bertinetti D, Diskar M, et al.** Stimulation of proglucagon gene expression by human GPR119 in enteroendocrine L-cell line GLUTag. *Mol Endocrinol*. 2013;27(8):1267–1282.
31. **Tsalkova T, Blumenthal DK, Mei FC, White MA, Cheng X.** Mechanism of Epac activation: structural and functional analyses of Epac2 hinge mutants with constitutive and reduced activities. *J Biol Chem*. 2009;284(35):23644–23651.
32. **Courilleau D, Bisserier M, Jullian JC, et al.** Identification of a tetrahydroquinoline analog as a pharmacological inhibitor of the cAMP-binding protein Epac. *J Biol Chem*. 2012;287(53):44192–44202.
33. **Cabrera O, Jacques-Silva MC, Speier S, et al.** Glutamate is a positive autocrine signal for glucagon release. *Cell Metab*. 2008;7(6):545–554.
34. **Schultz C.** Prodrugs of biologically active phosphate esters. *Bioorg Med Chem*. 2003;11(6):885–898.
35. **Jessen HJ, Schulz T, Balzarini J, Meier C.** Bioreversible protection of nucleoside diphosphates. *Angew Chem Int Ed Engl*. 2008; 47(45):8719–8722.
36. **Allen MD, Zhang J.** Subcellular dynamics of protein kinase A activity visualized by FRET-based reporters. *Biochem Biophys Res Commun*. 2006;348(2):716–721.
37. **Göke R, Fehmann HC, Linn T, et al.** Exendin-4 is a high potency agonist and truncated exendin-(9–39)-amide an antagonist at the glucagon-like peptide 1-(7–36)-amide receptor of insulin-secreting β-cells. *J Biol Chem*. 1993;268(26):19650–19655.
38. **Holz GG, Chepurny OG.** Glucagon-like peptide-1 synthetic analogs: new therapeutic agents for use in the treatment of diabetes mellitus. *Curr Med Chem*. 2003;10(22):2471–2483.
39. **de Rooij J, Zwartkruis FJ, Verheijen MH, et al.** Epac is a Rap1 guanine-nucleotide-exchange factor directly activated by cyclic AMP. *Nature*. 1998;396(6710):474–477.
40. **Kawasaki H, Springett GM, Mochizuki N, et al.** A family of cAMP-

binding proteins that directly activate Rap1. *Science*. 1998; 282(5397):2275–2279.
41. **Vliem MJ, Ponsioen B, Schwede F, et al.** 8-pCPT-2′-*O*-Me-cAMP-AM: an improved Epac-selective cAMP analogue. *Chembiochem*. 2008;9(13):2052–2054.
42. **Chepurny OG, Leech CA, Kelley GG, et al.** Enhanced Rap1 activation and insulin secretagogue properties of an acetoxymethyl ester of an Epac-selective cyclic AMP analog in rat INS-1 cells: studies with 8-pCPT-2′-*O*-Me-cAMP-AM. *J Biol Chem*. 2009;284(16): 10728–10736.
43. **Enserink JM, Christensen AE, de Rooij J, et al.** A novel Epac-specific cAMP analogue demonstrates independent regulation of Rap1 and ERK. *Nat Cell Biol*. 2002;4(11):901–906.
44. **Holz GG, Chepurny OG, Schwede F.** Epac-selective cAMP analogs: new tools with which to evaluate the signal transduction properties of cAMP-regulated guanine nucleotide exchange factors. *Cell Signal*. 2008;20(1):10–20.
45. **Rehmann H, Schwede F, Døskeland SO, Wittinghofer A, Bos JL.** Ligand-mediated activation of the cAMP-responsive guanine nucleotide exchange factor Epac. *J Biol Chem*. 2003;278(40):38548–3856.
46. **Kang G, Joseph JW, Chepurny OG, et al.** Epac-selective cAMP analog 8-pCPT-2′-*O*-Me-cAMP as a stimulus for Ca^{2+}-induced Ca^{2+} release and exocytosis in pancreatic β-cells. *J Biol Chem*. 2003;278(10):8279–8285.
47. **Seino S, Shibasaki T.** PKA-dependent and PKA-independent pathways for cAMP-regulated exocytosis. *Physiol Rev*. 2005;85(4): 1303–1342.
48. **Hatakeyama H, Kishimoto T, Nemoto T, Kasai H, Takahashi N.** Rapid glucose sensing by protein kinase A for insulin exocytosis in mouse pancreatic islets. *J Physiol*. 2006;570(pt 2):271–282.
49. **Hatakeyama H, Takahashi N, Kishimoto T, Nemoto T, Kasai H.** Two cAMP-dependent pathways differentially regulate exocytosis of large dense-core and small vesicles in mouse β-cells. *J Physiol*. 2007;582(pt 3):1087–1098.
50. **Leech CA, Chepurny OG, Holz GG.** Epac2-dependent Rap1 activation and the control of islet insulin secretion by glucagon-like peptide-1. *Vitam Horm*. 2010;84:279–302.
51. **Leech CA, Dzhura I, Chepurny OG, et al.** Molecular physiology of glucagon-like peptide-1 insulin secretagogue action in pancreatic β cells. *Prog Biophys Mol Biol*. 2011;107(2):236–247.
52. **Song WJ, Seshadri M, Ashraf U, et al.** Snapin mediates incretin action and augments glucose-dependent insulin secretion. *Cell Metab*. 2011;13(3):308–319.
53. **Tengholm A.** Cyclic AMP dynamics in the pancreatic β-cell. *Ups J Med Sci*. 2012;117(4):355–369.
54. **Kai AK, Lam AK, Chen Y, et al.** Exchange protein activated by cAMP 1 (Epac1)-deficient mice develop β-cell dysfunction and metabolic syndrome. *FASEB J*. 2013;27(10):4122–4135.
55. **Henquin JC, Nenquin M.** Activators of PKA and Epac distinctly influence insulin secretion and cytosolic Ca^{2+} in female mouse islets stimulated by glucose and tolbutamide. *Endocrinology*. 2014; 155(9):3274–3287.
56. **Takahashi N, Kadowaki T, Yazaki Y, Ellis-Davies GC, Miyashita Y, Kasai H.** Post-priming actions of ATP on Ca^{2+}-dependent exocytosis in pancreatic β cells. *Proc Natl Acad Sci USA*. 1999;96(2): 760–765.
57. **Leech CA, Dzhura I, Chepurny OG, Schwede F, Genieser HG, Holz GG.** Facilitation of β-cell K_{ATP} channel sulfonylurea sensitivity by a cAMP analog selective for the cAMP-regulated guanine nucleotide exchange factor Epac. *Islets*. 2010;2(2):72–81.
58. **Holz GG, Leech CA, Chepurny OG.** New insights concerning the molecular basis for defective glucoregulation in soluble adenylyl cyclase knockout mice. *Biochim Biophys Acta*. 2014;1842(12 pt B):2593–2600.
59. **Takahashi N, Nemoto T, Kimura R, et al.** Two-photon excitation imaging of pancreatic islets with various fluorescent probes. *Diabetes*. 2002;51(suppl 1):S25–S28.
60. **Ma YH, Wang J, Rodd GG, Bolaffi JL, Grodsky GM.** Differences in insulin secretion between the rat and mouse: role of cAMP. *Eur J Endocrinol*. 1995;132(3):370–376.
61. **Waeber G, Calandra T, Roduit R, et al.** Insulin secretion is regulated by the glucose-dependent production of islet β cell macrophage migration inhibitory factor. *Proc Natl Acad Sci USA*. 1997; 94(9):4782–4787.
62. **Kawai J, Ohara-Imaizumi M, Nakamichi Y, et al.** Insulin exocytosis in Goto-Kakizaki rat β-cells subjected to long-term glinide or sulfonylurea treatment. *Biochem J*. 2008;412(1):93–101.
63. **Persaud SJ, Jones PM, Howell SL.** Glucose-stimulated insulin secretion is not dependent on activation of protein kinase A. *Biochem Biophys Res Commun*. 1990;173(3):833–839.
64. **Sato Y, Henquin JC.** The K-ATP channel-independent pathway of regulation of insulin secretion by glucose: in search of the underlying mechanism. *Diabetes*. 1998;47(11):1713–1721.
65. **Harris TE, Persaud SJ, Jones PM.** Pseudosubstrate inhibition of cyclic AMP-dependent protein kinase in intact pancreatic islets: effects on cyclic AMP-dependent and glucose-dependent insulin secretion. *Biochem Biophys Res Commun*. 1997;232(3):648–651.
66. **Lester LB, Langeberg LK, Scott JD.** Anchoring of protein kinase A facilitates hormone-mediated insulin secretion. *Proc Natl Acad Sci USA*. 1997;94(26):14942–14947.
67. **Henquin JC.** Triggering and amplifying pathways of regulation of insulin secretion by glucose. *Diabetes*. 2000;49(11):1751–1760.
68. **Henquin JC, Ishiyama N, Nenquin M, Ravier MA, Jonas JC.** Signals and pools underlying biphasic insulin secretion. *Diabetes*. 2002;51(suppl 1):S60–S67.
69. **Henquin JC.** The dual control of insulin secretion by glucose involves triggering and amplifying pathways in β-cells. *Diabetes Res Clin Pract*. 2011;93(suppl 1):S27–S31.
70. **Dzhura I, Chepurny OG, Kelley GG, et al.** Epac2-dependent mobilization of intracellular Ca^{2+} by glucagon-like peptide-1 receptor agonist exendin-4 is disrupted in β-cells of phospholipase C-ε knockout mice. *J Physiol*. 2010;588(pt 24):4871–4889.
71. **Dzhura I, Chepurny OG, Leech CA, et al.** Phospholipase C-ε links Epac2 activation to the potentiation of glucose-stimulated insulin secretion from mouse islets of Langerhans. *Islets*. 2011;3(3):121–128.
72. **Smrcka AV, Brown JH, Holz GG.** Role of phospholipase Cε in physiological phosphoinositide signaling networks. *Cell Signal*. 2012;24(6):1333–1343.
73. **Dyachok O, Idevall-Hagren O, Sågetorp J, et al.** Glucose-induced cyclic AMP oscillations regulate pulsatile insulin secretion. *Cell Metab*. 2008;8(1):26–37.
74. **Idevall-Hagren O, Barg S, Gylfe E, Tengholm A.** cAMP mediators of pulsatile insulin secretion from glucose-stimulated single β-cells. *J Biol Chem*. 2010;285(30):23007–23018.
75. **Idevall-Hagren O, Jakobsson I, Xu Y, Tengholm A.** Spatial control of Epac2 activity by cAMP and Ca^{2+}-mediated activation of Ras in pancreatic β cells. *Sci Signal*. 2013;6(273):ra29.1–11, S1–S6.
76. **Tian G, Sandler S, Gylfe E, Tengholm A.** Glucose- and hormone-induced cAMP oscillations in α- and β-cells within intact pancreatic islets. *Diabetes*. 2011;60(5):1535–1543.
77. **Tian G, Sol ER, Xu Y, Shuai H, Tengholm A.** Impaired cAMP generation contributes to defective glucose-stimulated insulin secretion after long-term exposure to palmitate. *Diabetes*. 2015;64(3): 904–915.
78. **Landa LR Jr, Harbeck M, Kaihara K, et al.** Interplay of Ca^{2+} and cAMP signaling in the insulin-secreting MIN6 β-cell line. *J Biol Chem*. 2005;280(35):31294–31302.
79. **Fridlyand LE, Harbeck MC, Roe MW, Philipson LH.** Regulation of cAMP dynamics by Ca^{2+} and G protein-coupled receptors in the pancreatic β-cell: a computational approach. *Am J Physiol Cell Physiol*. 2007;293(6):C1924–C1933.

80. **Holz GG, Heart E, Leech CA.** Synchronizing Ca^{2+} and cAMP oscillations in pancreatic β-cells: a role for glucose metabolism and GLP-1 receptors? Focus on "regulation of cAMP dynamics by Ca^{2+} and G protein-coupled receptors in the pancreatic β-cell: a computational approach". *Am J Physiol Cell Physiol*. 2008;294(1):C4–C6.
81. **Takeda Y, Amano A, Noma A, Nakamura Y, Fujimoto S, Inagaki N.** Systems analysis of GLP-1 receptor signaling in pancreatic β-cells. *Am J Physiol Cell Physiol*. 2011;301(4):C792–C803.
82. **Hodson DJ, Mitchell RK, Marselli L, et al.** ADCY5 couples glucose to insulin secretion in human islets. *Diabetes*. 2014;63(9):3009–3021.
83. **Zippin JH, Chen Y, Straub SG, et al.** CO_2/HCO_3^-- and calcium-regulated soluble adenylyl cyclase as a physiological ATP sensor. *J Biol Chem*. 2013;288(46):33283–33291.
84. **Song WJ, Mondal P, Li Y, Lee SE, Hussain MA.** Pancreatic β-cell response to increased metabolic demand and to pharmacologic secretagogues requires EPAC2A. *Diabetes*. 2013;62(8):2796–2807.
85. **Holz GG, Chepurny OG, Leech CA.** Epac2A makes a new impact in β-cell biology. *Diabetes*. 2013;62(8):2665–2666.
86. **Shibasaki T, Takahashi H, Miki T, et al.** Essential role of Epac2/Rap1 signaling in regulation of insulin granule dynamics by cAMP. *Proc Natl Acad Sci USA*. 2007;104(49):19333–19338.
87. **Gaisano HY.** Here come the newcomer granules, better late than never. *Trends Endocrinol Metab*. 2014;25(8):381–388.
88. **Christensen AE, Selheim F, de Rooij J, et al.** cAMP analog mapping of Epac1 and cAMP kinase. Discriminating analogs demonstrate that Epac and cAMP kinase act synergistically to promote PC-12 cell neurite extension. *J Biol Chem*. 2003;278(37):35394–35402.
89. **Brown LM, Rogers KE, McCammon JA, Insel PA.** Identification and validation of modulators of exchange protein activated by cAMP (Epac) activity: structure-function implications for Epac activation and inhibition. *J Biol Chem*. 2014;289(12):8217–8230.
90. **Skelin M, Rupnik M.** cAMP increases the sensitivity of exocytosis to Ca^{2+} primarily through protein kinase A in mouse pancreatic β cells. *Cell Calcium*. 2011;49(2):89–99.
91. **Brunzell JD, Robertson RP, Lerner RL, et al.** Relationships between fasting plasma glucose levels and insulin secretion during intravenous glucose tolerance tests. *J Clin Endocrinol Metab*. 1976;42(2):222–229.
92. **Gerich JE.** Is reduced first-phase insulin release the earliest detectable abnormality in individuals destined to develop type 2 diabetes? *Diabetes*. 2002;51(suppl 1):S117–S121.
93. **Seino S, Shibasaki T, Minami K.** Dynamics of insulin secretion and the clinical implications for obesity and diabetes. *J Clin Invest*. 2011;121(6):2118–2125.
94. **Nadkarni P, Chepurny OG, Holz GG.** Regulation of glucose homeostasis by GLP-1. *Prog Mol Biol Transl Sci*. 2014;121:23–65.
95. **Holz GG, Leech CA, Roe MW, Chepurny OG.** High-throughput FRET assays for fast time-dependent detection of cyclic AMP in pancreatic β cells. In: Cheng X, ed. *Cyclic Nucleotide Signaling*, Boca Raton, FL: CRC Press; 2015:35–59.
96. **Groenewoud MJ, Dekker JM, Fritsche A, et al.** Variants of CDKAL1 and IGF2BP2 affect first-phase insulin secretion during hyperglycaemic clamps. *Diabetologia*. 2008;51(9):1659–1663.
97. **Simonis-Bik AM, Eekhoff EM, de Moor MH, et al.** Genetic influences on the insulin response of the β cell to different secretagogues. *Diabetologia*. 2009;52(12):2570–2577.
98. **'t Hart LM, Simonis-Bik AM, Nijpels G, et al.** Combined risk allele score of eight type 2 diabetes genes is associated with reduced first-phase glucose-stimulated insulin secretion during hyperglycemic clamps. *Diabetes*. 2010;59(1):287–292.